Siting Solar Photovoltaics on Distribution Feeders: Comparing deployment models and their limits

Anna Brockway

Electrical Engineering and Computer Sciences
University of California at Berkeley

Technical Report No. UCB/EECS-2020-192
http://www2.eecs.berkeley.edu/Pubs/TechRpts/2020/EECS-2020-192.html

December 1, 2020

Copyright © 2020, by the author(s).
All rights reserved.

Permission to make digital or hard copies of all or part of this work for personal or classroom use is granted without fee provided that copies are not made or distributed for profit or commercial advantage and that copies bear this notice and the full citation on the first page. To copy otherwise, to republish, to post on servers or to redistribute to lists, requires prior specific permission.

Acknowledgement

I am grateful to Mingxi Liu for help formulating the problem setup and members of the Energy Modeling, Control, and Analysis research group for early feedback on the project and its scope. Phillippe Phanivong and Antoine Lesage-Landry kindly helped trouble-shoot aspects of the methodology and analysis. I am grateful to my readers, Duncan Callaway and Kameshwar Poolla, for engaging thoughtfully with this work and providing valuable feedback.

Siting Solar Photovoltaics on Distribution Feeders

Comparing deployment models and their limits

Anna Brockway
Master's Project, December 2019
Electrical Engineering and Computer Sciences
University of California, Berkeley

Abstract

The deployment of solar photovoltaic arrays on electric distribution grids carries ramifications for grid reliability, power quality, and operations. Safely accommodating solar PV can aid renewable energy deployment goals and potentially provide grid benefits. Here, we assess the technical limits to PV deployment on distribution feeders by comparing the characteristics of two real-world deployment models: residential rooftop solar and community solar. We assess the potential to maximize the deployment of these two models in the context of allowable voltages on a distribution system. We find that enabling community solar deployment, either in addition to or instead of rooftop solar, can substantially increase the amount of solar a distribution feeder can accommodate.

Index Terms

Solar photovoltaics, distribution feeders, voltage constraints, community solar, residential rooftop solar.

I. Introduction and Motivation

Customer-facing solar is growing rapidly on California's distribution feeders. However, the limits to the distribution system's ability to accommodate solar are not well understood. A commonly invoked rule of thumb is that a distribution feeder can accommodate up to 15% of its peak load without issue [1]. In practice, there is wide variation among feeders [2]. Moreover, how solar physically looks on the grid (i.e., size, location, presence or absence of accompanying equipment such as storage, tracking systems, and smart inverters) impacts how it integrates with the system [3], [4].

Beyond their technical implications, solar deployment models also carry implications for policymakers and regulators. Behind-the-meter solar has become a key contributor to helping California meet its renewable energy targets [5] and part of the strategy for future deployment [6]. Yet concerns about feeder impacts and possible limits to deployment have prompted regulatory processes and intensive working groups to better understand hosting capacity and its implications [7]. The choice to adopt residential rooftop solar largely rests with individual homeowners, and is often spurred on by strong financial incentives [8]. Yet while behind-the-meter residential solar PV has grown to over 5 gigawatts of installed capacity [9], little coherent policy exists in the state on other distributed deployment models; most notably, community solar [10]. Community solar has different physical characteristics that may carry implications for electricity grid impacts and, therefore, for renewable energy deployment goals.

Here, we seek to assess the system constraints to deploying solar on distribution circuits through the lens of these two real-world deployment models. Residential rooftop solar is deployed in small arrays, approx. 3-7 kW each, and placed relatively randomly throughout a distribution feeder. Community solar is deployed in larger arrays, approx.

10 kW-1 MW, and has the potential to be sited with input from the grid operator [11]. Community solar also has greater economies of scale and flexibility in compensation mechanisms, potentially enabling experimentation with accompanying equipment and control schemes.

We use deployment characteristics of these two business models as a framework to test the limits to solar integration on distribution feeders. Specifically, we seek to maximize the amount of solar that can be deployed on distribution feeders without violating voltage limits. This approach streamlines an array of theoretical design choices for DERs into options that are practically possible today. Our aim is to perform a novel engineering assessment with realistic solar deployment scenarios and to compare the technical impacts of policy-relevant deployment models.

II. Methods

A. Translating realistic characteristics of solar deployment models into simulation scenarios

Customer load and solar data are obtained from public data sources and cleaned via R (version 3.6.1).

1) Geographies: We select three locations for comparison within the state of California. Sacramento, Berkeley, and Los Angeles are located in different California climate zones with varying weather conditions, solar potential, and residential load profiles (Table I). We focus on Sacramento for now and leave the other two locations for future work.

2) Customer loads: Simulated energy use profiles for residential customers are available for typical meteorological year (TMY) data for many locations across the United States [12]. These data contain estimates for energy consumption by low-, base-, and high-energy users. We rely on colleagues' previous analysis to estimate the proportion of residential customers in each of the three geographic areas of interest that fall into these different tiers [13] (Table I). We use values for all customers, not just those residing in single-family homes, as all residential customers could conceivably offset their energy use through either rooftop or community solar. Moreover, the load profile of all customers will contribute to the voltage profile of the distribution feeder. The load profiles for Sacramento used in this analysis are visualized in Figure 1.

TABLE I
GEOGRAPHIC LOCATIONS

City	California Climate Zones ([14], [15])				TMY3 Load Profiles [12]				
	CZ	Reference Locations	HDD* (base=65F)	CDD* (base=80F)	Reference Locations (Airports)	County FIPS Code	Customers in Usage Tier (%) [13]		
							LOW	BASE	HIGH
Sacramento	12	Stockton	2702	1470	SAC	067	0.37	0.40	0.23
Berkeley	3	OAK	2909	128	OAK	001	0.18	0.32	0.50
Los Angeles	6	LAX	1458	727	LAX	037	0.35	0.39	0.26

*HDD and CDD refer to Heating Degree Days and Cooling Degree Days and are defined as "the summation of degrees of the average temperature per day for the year" above 80 degrees F or below 65 degrees F, respectively [15].

3) Solar power production: The amount of electricity that a solar array sends into the electric grid depends on several factors, including the material used in the PV cells, the amount of incident solar radiation (which varies with weather, time of day, and season), and the location and orientation of the panels [16]. Here, we use the National Renewable Energy Laboratory's PVWatts tool to estimate the amount of power produced from PV arrays located in Sacramento [17]. We consider two primary cases of solar deployment: residential rooftop and community solar.

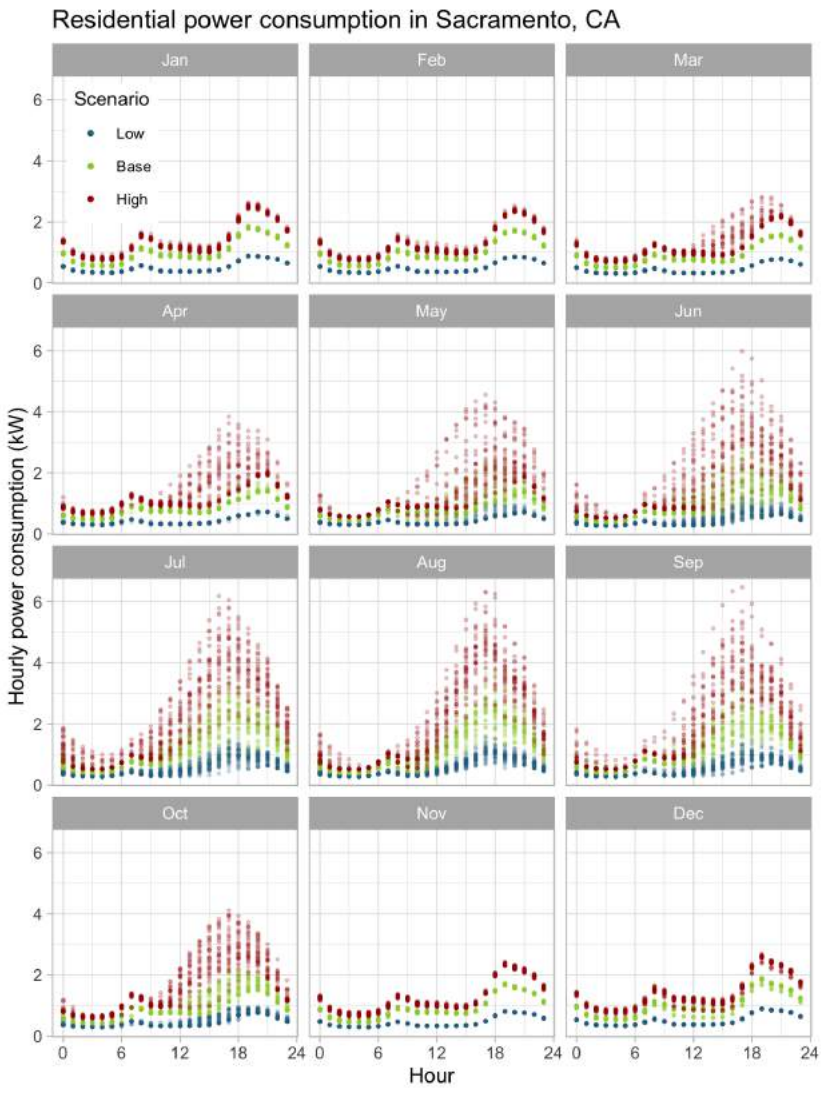

Fig. 1. Hourly load profiles for residential customers in Sacramento by month.

a) Irradiance data: PVWatts uses data from the National Solar Radiation Database to calculate solar production on the basis of irradiance and other weather conditions. A recent update involved a full revamping of the underlying methodology, moving from extrapolating conditions from empirical data to a "physics-based modeling approach" [18]. We use the TMY estimate of this irradiance data for input into PVWatts.

b) Residential rooftop solar: Residential arrays are typically fixed to customer rooftops, with tilt and azimuth depending on available roof space and orientation. The power production from these arrays depends heavily on module tilt and orientation (Figure 2). We focus on the highest-production orientation (tilt 30 deg., azimuth 180 deg.) in the present study, and leave the mix of solar scenarios for future work. However, we do use solar installation data from Tracking the Sun [19] to estimate a realistic mix of tilt and azimuth characteristics for residential rooftop solar installations (Figures 3a and 3b), and propose a weighting to apply to residential systems (Figure 3c).

c) Community solar: Community arrays can be ground-mounted or fixed to rooftops. For simplicity, we consider only ground-mounted scenarios with unlimited capacity sited at one system location (node). We choose the base tilt (30 deg from horizontal) and azimuth (180 deg clockwise from true north) for community PV based on the highest-production orientation from rooftop PV data (Figure 2a). We consider a second scenario with panels

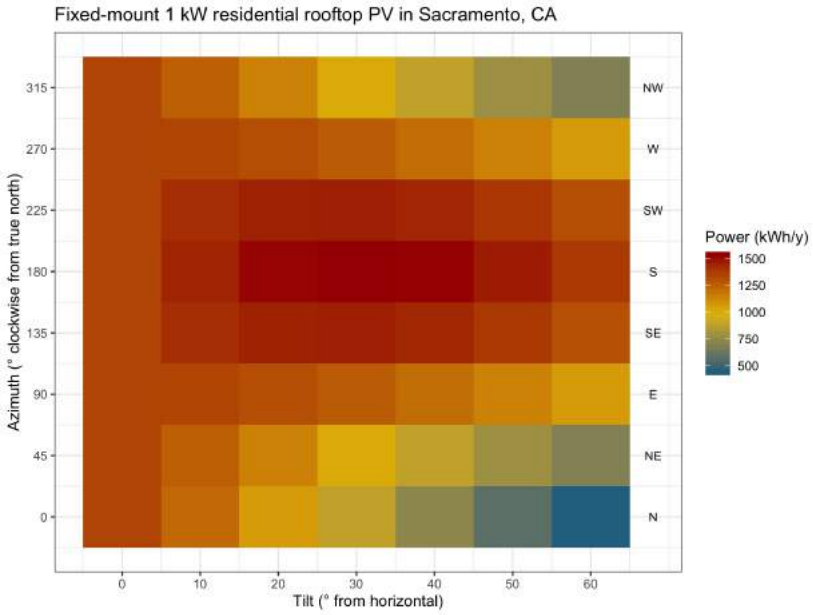

(a)

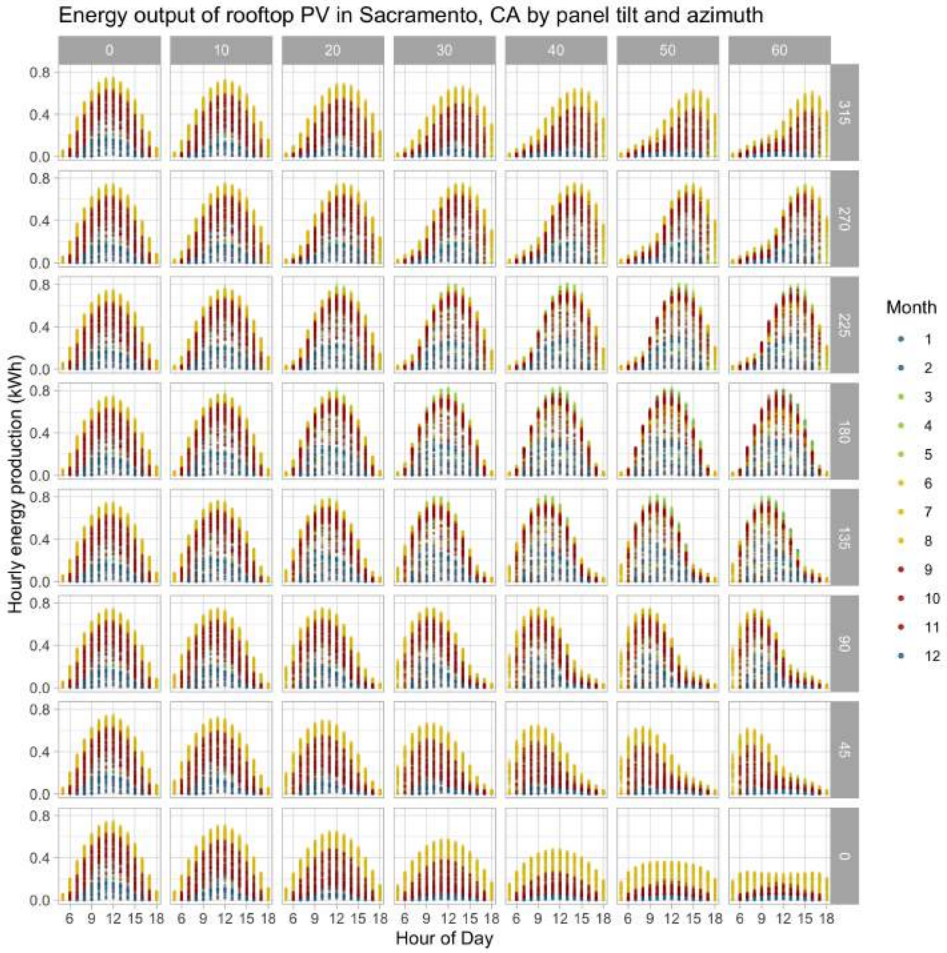

(b)

Fig. 2. (a) Annual and (b) hourly rooftop PV production by tilt and azimuth in Sacramento, CA.

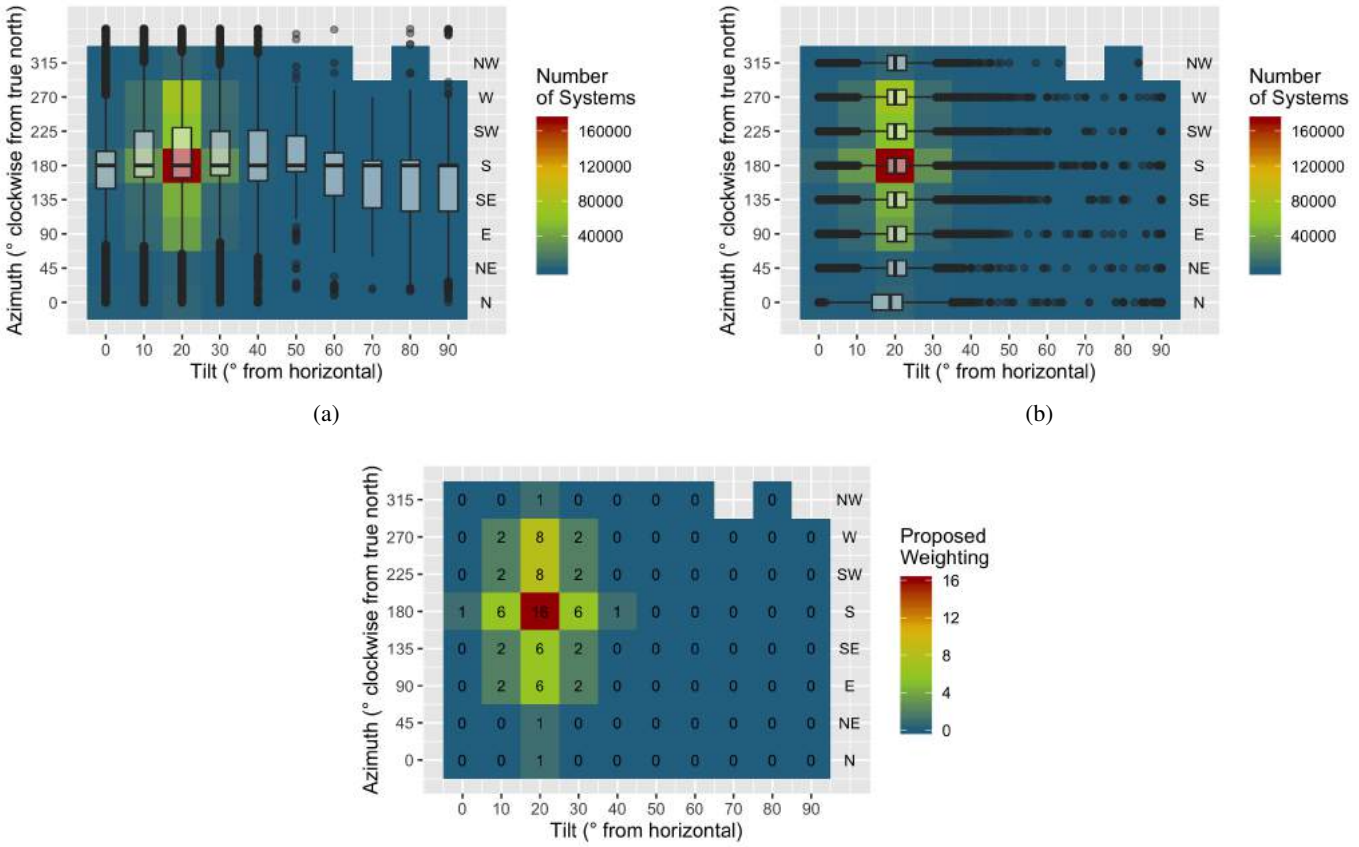

Fig. 3. Range of tilt and azimuth scenarios for residential rooftop PV within the public data file released with the 2019 Tracking the Sun report [19]. Visualizations shown here were calculated from 560,914 PV systems installed for residential customers, located in California, not ground-mounted, sized at less than or equal to 20 kW, and possessing both tilt and azimuth information. Box-and-whisker plots are shown to indicate medians, quartiles, and outliers for (a) azimuth given a tilt category and (b) tilt given an azimuth category. On the basis of these data, we propose weights for these tilt and azimuth categories to assign to residential PV arrays. These are visualized in (c).

oriented to the southwest for greater afternoon sun exposure. We also consider community arrays equipped with 1-axis tracking (with backtracking to reduce shading impacts). We simulate these scenarios with an initial tilt of zero degrees (flat panels) and south- and southwest-facing azimuth orientations. The annual and hourly power production from these four scenarios are visualized in Figure 4. Each scenario will be evaluated independently.

d) Additional details: All PVWatts scenarios are run for PV arrays assuming standard modules with estimated system losses of 14.08%. Scenarios are summarized in Table II.

4) Analysis timeframe: Solar production and customer loads exhibit seasonal as well as daily variation. We consider two types of temporal data for analysis: (a) all 8760 hours of a typical meteorological year, and (b) average hours ('avghrs', 12×24) of each month of that year. Averaging the solar, load, and voltage conditions across days in a given month preserves seasonal fluctuations while smoothing out daily extremes. We examine this data for context about overall seasonal patterns in feeder conditions. Increasing storage adoption and demand response adoption could, over time, smooth out daily and hourly fluctuations and move actual feeder conditions closer to these broader seasonal trends. However, as voltage conditions on electrical grids are strongly affected by hourly and sub-hourly fluctuations, considering daily extremes is necessary for solar deployment today. We expect that relative extremes will set limits on the amount of solar that can be deployed on the system, so the average

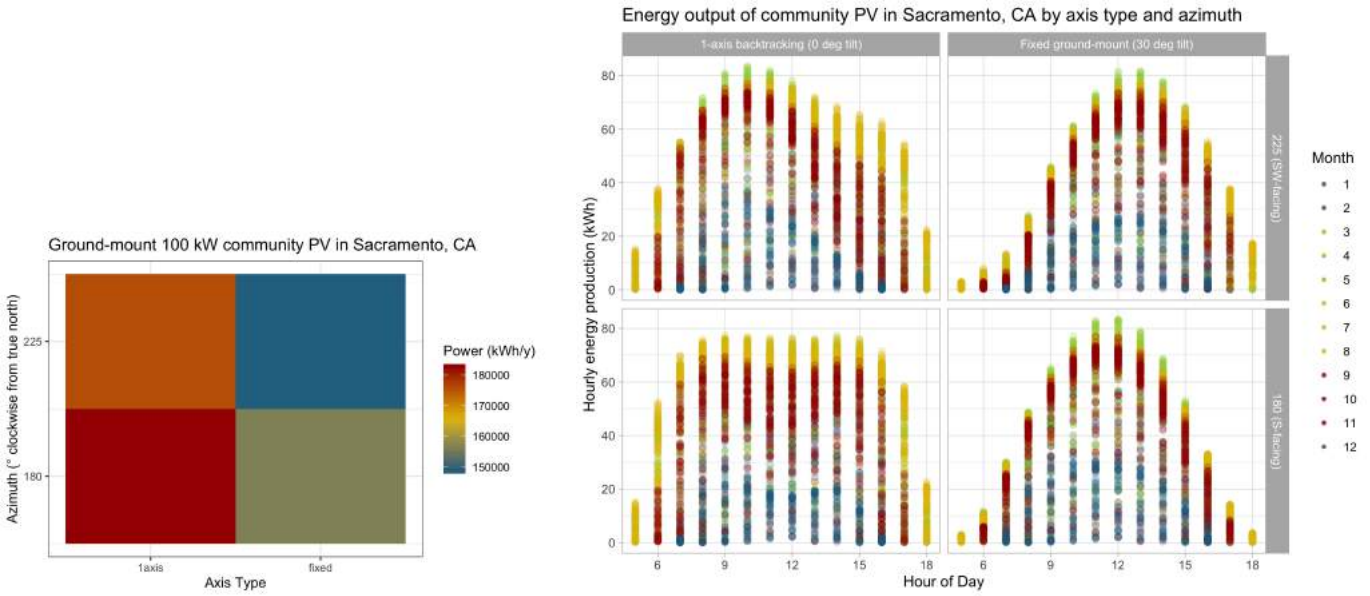

(a) (b)

Fig. 4. Annual and hourly energy production for community solar scenarios.

TABLE II
SUMMARY OF SOLAR DEPLOYMENT SCENARIOS

Solar type	Scenario	Details	Constraints
(A) All residential rooftop	(1) All systems at 30 deg. tilt, 180 deg. azimuth (2) Mix of tilts and azimuths, orientations randomly assigned to houses (see weighting in Figure 3c), left for future work	Fixed roof mount, standard module, estimated system losses of 14.08%	Annual production may not exceed power consumption (net metering constraint)
(B) All community solar	(1) Fixed axis, 30 deg. tilt, (a) 180 deg. azimuth and (b) 225 deg. azimuth (2) 1-axis tracking (with backtracking), 0 deg. tilt, (a) 180 deg. azimuth and (b) 225 deg. azimuth	Ground mount, standard module, estimated system losses of 14.08%	Deployed at one node, no upper limit on size
(C) Mix of residential rooftop and community solar	(1) Scenarios A1 and B1a (2) Scenarios A1 and B2b		

hour conditions will allow more capacity to be built. The difference in capacity deployment between these two conditions will provide insight about the contribution of daily fluctuations to deployment limits.

B. Distribution feeder setup and DistFlow formulation

We use Matlab R2018b for feeder setup and calculations.

1) Distribution feeder model and allowable voltage: We use the IEEE 13-bus test feeder with 12 nodes [20], [21]. The feeder's operating voltage is 4.16 kV. We consider a single-phase version of this feeder and set our base voltage to:

$$v_0 = \frac{4160}{\sqrt{3}} = 2401.8V \tag{1}$$

Following ANSI standards, service voltage is allowed to fluctuate 5% from its base value [22], [23]. The allowable voltage range here is thus 2281.7 to 2521.9 volts (0.95 to 1.05 p.u.). Squared values, used in voltage magnitude calculations (Section II-B3), are 5.7685×10^6 volts^2 for a starting base value and 5.2061×10^6 and 6.3598×10^6 volts^2 for lower and upper bounds, respectively.

We assemble the distribution network model as discussed in [24]. We compare three different variants of this feeder: (a) the full feeder, with 12 nodes available for load and solar, (b) a 'near' case of five nodes closer to the substation head, and (c) a 'far' case of five nodes branching out to the ends of the feeder (Figure 5). Where variants are considered, we keep only the portions of the R and X matrices corresponding to those nodes and line segments.

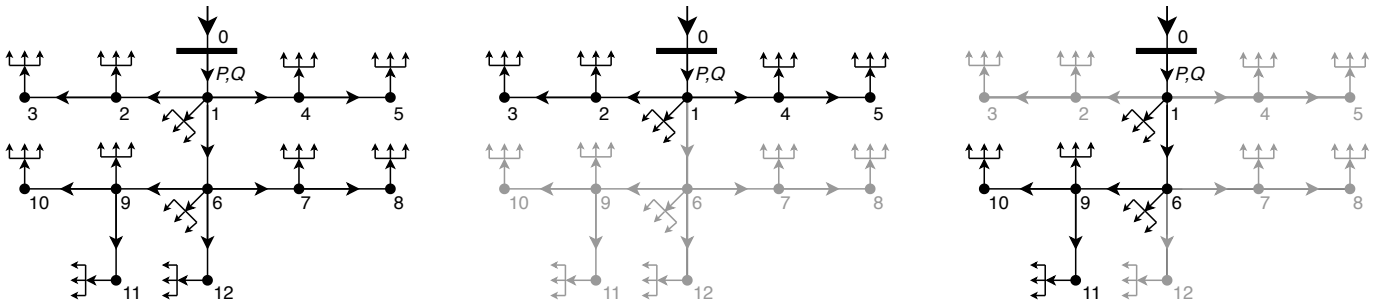

(a) (b) (c)

Fig. 5. IEEE13 feeder variants considered in this work: (a) full feeder, (b) 'near' case of nodes 1-5, and (c) 'far' case of nodes 1, 6, and 9-11. The greyed-out sections of (b) and (c) are omitted from analysis. Arrows symbolize flows of real and reactive power.

2) Real and reactive power: We explicitly consider three separate types of power flows. Real power demand by residential customers is calculated via assigned load profiles (Section II-A2). Reactive power demand by residential customers is calculated from real power demand assuming a 0.9 static power factor. Real power generated by solar arrays is calculated via solar production profiles (Section II-A3) and deployed capacity. (Future work will also consider reactive power support by solar inverters.)

3) Voltage dynamics and losses: In a simplified single-phase radial distribution feeder, we can describe power flow and voltage with the following equations [25], [26] (see Appendix A for a more thorough write-out and table

of symbols). For any node i and downstream nodes j:

$$P_i = p_i + \sum_j \left(P_j - r_{ij} \frac{P_{ij}^2 + Q_{ij}^2}{V_j^2} \right) \tag{2}$$

$$Q_i = q_i + \sum_j \left(Q_j - x_{ij} \frac{P_{ij}^2 + Q_{ij}^2}{V_j^2} \right) \tag{3}$$

$$|V_i|^2 = |V_j|^2 - 2r_{ij}P_j - 2x_{ij}Q_j + \left(r_{ij}^2 + x_{ij}^2\right) \left(\frac{P_{ij}^2 + Q_{ij}^2}{|V_j|^2} \right) \tag{4}$$

These equations are linear except for the loss terms. These can be represented as a second-order cone program (SOCP) to preserve convexity, as in [27]–[29]:

$$|V_i|^2 = |V_j|^2 - 2r_{ij}P_j - 2x_{ij}Q_j + \left(r_{ij}^2 + x_{ij}^2\right) loss_{ij} \tag{5}$$

$$loss_{ij}|V_j|^2 \geq P_{ij}^2 + Q_{ij}^2 \qquad \Longleftrightarrow \qquad loss_{ij} + |V_j|^2 \geq \left\| \begin{bmatrix} 2P_{ij} \\ 2Q_{ij} \\ loss_{ij} - |V_j|^2 \end{bmatrix} \right\| \tag{6}$$

Here, we formulate our problem by embedding the network information into R and X matrices and focusing on a nodal representation of the real and reactive power quantities, as in [24]. This nodal representation removes the line flow information, hindering our ability to explicitly consider line losses for now. (We will return to this in future work.) Collecting equations 2 through 4 for all n nodes in the network at a given discrete time k gives us the overall relationship:

$$V_k = V_0 - 2Rp_k - 2Xq_k \tag{7}$$

Where:

$$V_k = \begin{bmatrix} |V_{(1,k)}|^2 \\ |V_{(2,k)}|^2 \\ \vdots \\ |V_{(n,k)}|^2 \end{bmatrix}, \qquad V_0 = \begin{bmatrix} |V_{(0,k)}|^2 \\ |V_{(0,k)}|^2 \\ \vdots \\ |V_{(0,k)}|^2 \end{bmatrix}, \qquad p_k = \begin{bmatrix} p_{(1,k)} \\ p_{(2,k)} \\ \vdots \\ p_{(n,k)} \end{bmatrix}, \qquad q_k = \begin{bmatrix} q_{(1,k)} \\ q_{(2,k)} \\ \vdots \\ q_{(n,k)} \end{bmatrix}, \qquad R, X \in \mathbb{R}^{n \times n}$$

And:

$$R_{ij} = \sum_{(\hat{i},\hat{j}) \in E_i \cap E_j} r_{\hat{i},\hat{j}}$$

Where E_i is the set containing the line segments that connect node 0 to node i. This equation will be solved for each relevant hour k.

Including real power production from solar throughout the feeder, the overall equation becomes:

$$V_k = V_0 - 2R\left(p_{bk} - p_{sk}\right) - 2Xq_k \tag{8}$$

Since solar power production is a linear function of installed capacity at each node, we can determine the production from a given installed capacity by relating the DC system size to AC power output for every hour of the day:

$$V_k = V_0 - 2R\left(p_{bk} - p_{sk,1kW.} \times C_{kW}\right) - 2Xq_k \tag{9}$$

where the multiplication of $p_{sk,1kW}$ with C_{kW} occurs element-wise, and p_{bk}, $p_{sk,1kW}$, C_{kW} and q_k are vectors containing baseline real power consumption, solar power production from a 1 kW array, installed solar power

capacity (DC size, in kW), and baseline reactive power consumption, respectively, at each node at time k:

$$p_{bk} = \begin{bmatrix} p_{b(1,k)} \\ p_{b(2,k)} \\ \vdots \\ p_{b(n,k)} \end{bmatrix}, \qquad p_{sk,1kW} = \begin{bmatrix} p_{s(1,k)} \\ p_{s(2,k)} \\ \vdots \\ p_{s(n,k)} \end{bmatrix}, \qquad C_{kW} = \begin{bmatrix} C_{1,kW} \\ C_{2,kW} \\ \vdots \\ C_{n,kW} \end{bmatrix}, \qquad q_k = \begin{bmatrix} q_{(1,k)} \\ q_{(2,k)} \\ \vdots \\ q_{(n,k)} \end{bmatrix}$$

4) Load tap changer at the substation: A load tap changer (LTC) is a type of voltage regulator that is typically located at the substation. An LTC changes the turns ratio in its transformer windings via a tap change adjustment in order to raise or lower the system voltage in response to a voltage drop or increase at a node further away [30]. The voltage at the remote node may be monitored or estimated [23].

Here, we implement an LTC that monitors the voltage at node 6 for the full feeder and 'far' variant, and node 2 for the 'near' variant (Figure 5). If the monitored voltage is found to be lower or higher than the allowed tolerance, the LTC raises or lowers the voltage at node 0. The LTC can operate 16 steps in either direction (32 steps total), with each step equivalent to an adjustment of 0.0625 p.u., for a total of $\pm 10\%$ of the rated feeder voltage. The lower voltage tolerance for LTC operation is set to 0.955 p.u. to account for the estimated voltage drop between node 6 and nodes further along the feeder lines in the full feeder case. After each step change, the per-unit voltage is recalculated with reference to the original (not LTC-adjusted) voltage to test if the voltage remains out-of-bounds.

Here, the LTC is run to calculate the original base voltage due to the loading of the feeder. It is omitted from the optimization step for now. (We will return to this in future work.) Another simplification is that we record the operation of the LTC but do not assign any penalty to step changes. In real systems, too-frequent LTC operation carries drawbacks as it can lead to more wear-and-tear and shorter equipment lifetimes [30].

C. Incorporating system dynamics and constraints

The optimization is implemented in Matlab R2018b with YALMIP [31]. We use Matlab's matrix and cell array architecture to keep track of matrices involved in the calculations. Hourly matrices are structured to track hourly values for each month and day of the year and average hour values for each month of the year (Figure 6a). These are used in voltage and power flow calculations. House matrices are structured to track house-level values (Figure 6b) and are used for the net metering constraints.

In this matrix notation, Equation 9 becomes:

$$\underbrace{V}_{\text{N\_node}\times\text{N\_hr}} = \underbrace{V_0}_{\text{N\_node}\times\text{N\_hr}} - 2 \underbrace{R}_{\text{N\_node}\times\text{N\_node}} \left(\underbrace{P_b}_{\text{N\_node}\times\text{N\_hr}} - \underbrace{P_{s,1kW}}_{\text{N\_node}\times\text{N\_hr}} .\times \underbrace{C_{kW}}_{\text{N\_node}\times 1} \right) - 2 \underbrace{X}_{\text{N\_node}\times\text{N\_node}} \underbrace{Q_b}_{\text{N\_node}\times\text{N\_hr}} \tag{10}$$

$$\underbrace{V}_{\text{N\_node}\times\text{N\_hr}} = \underbrace{V_0}_{\text{N\_node}\times\text{N\_hr}} - 2 \underbrace{R}_{\text{N\_node}\times\text{N\_node}} \left(\underbrace{P_b}_{\text{N\_node}\times\text{N\_hr}} - \underbrace{C_{kW}}_{\text{N\_node}\times 1} \times \underbrace{P_{sc,1kW}}_{1\times\text{N\_hr}} \right) - 2 \underbrace{X}_{\text{N\_node}\times\text{N\_node}} \underbrace{Q_b}_{\text{N\_node}\times\text{N\_hr}} \tag{11}$$

where Equations 10 and 11 calculate the voltage across the feeder at each node and each evaluated hour for residential and community solar, respectively. For residential solar, the multiplication of $P_{s,1kW}$ and C_{kW} occurs element-wise (by vector column). For community solar, the vector C_{kW} denotes at which node the solar array is sited. There is only one hourly profile ($P_{sc,1kW}$) as only one node at a time hosts community solar.

1) Assigning load to feeder nodes: We create a matrix `allo_load` ($N\_node \times hpernode$) that contains a random assignment of load classes for each house on the feeder. Load classes (1, 2, and 3) correspond to low-,

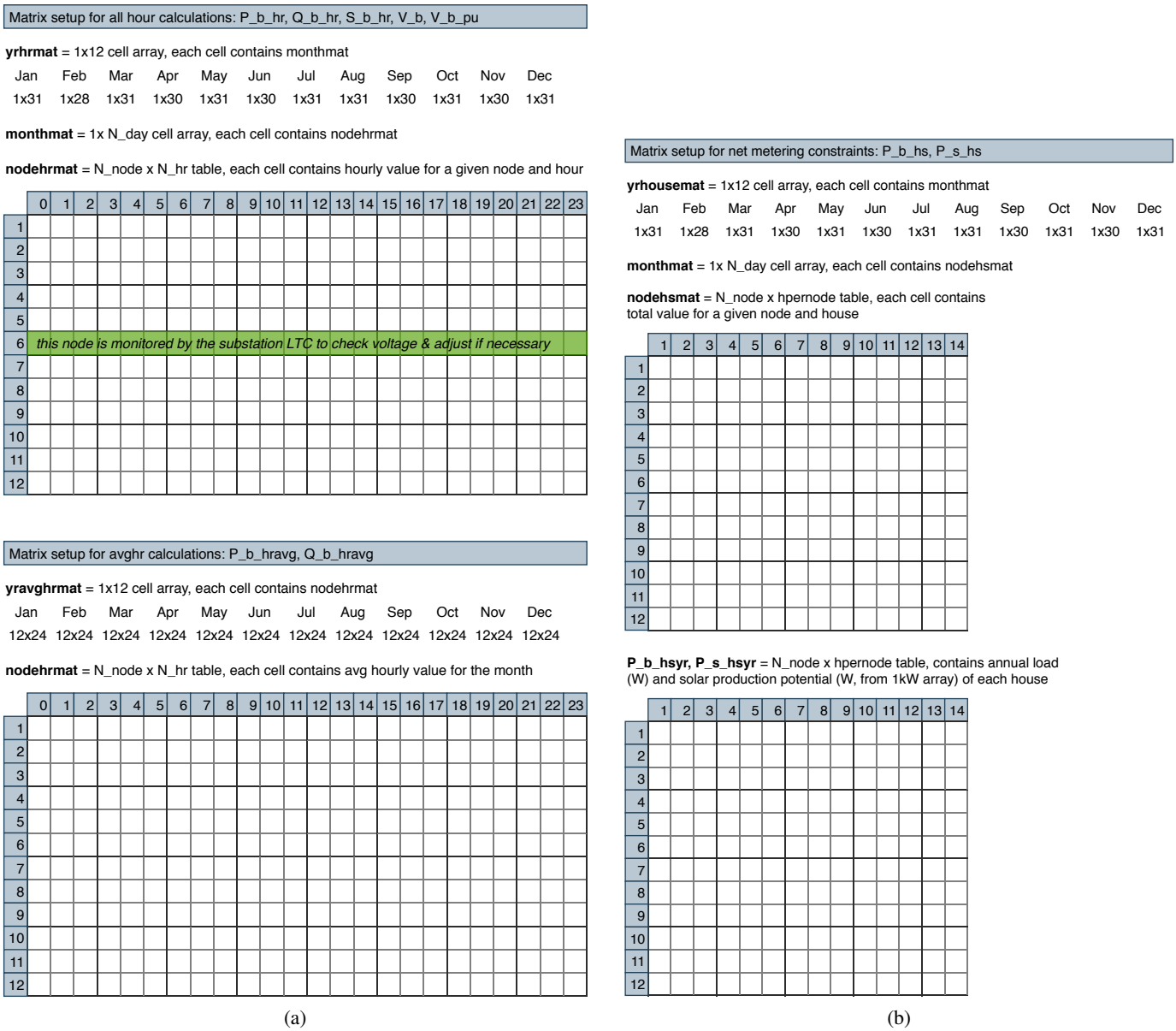

Fig. 6. Matrix setup for calculations and optimization. Matrices in (a) keep track of hourly power and voltage variables at each node of the feeder, either for each month and day of the year (top), or for average hours of each month of the year (bottom). Matrices in (b) keep track of house-level power variables at each node and house of the feeder (shown here assuming 14 houses per node).

base-, and high-energy use customers. The random assignment is weighted by the percentage of customers per usage tier (Table I). We build up the matrices `P_b_hr` and `P_b_hs` by assigning the hourly load for the selected customer type to each hour and house on the feeder, respectively. We calculate the baseline voltage for all hours of the year and average hours via Equation 8 without any solar on the system but with operating LTC.

We check voltage at all hours, voltage at average hours by month, and LTC operation under different loading scenarios (i.e., houses per node) (Figure 7). We find that 14 houses is the highest allowable number per node for the full feeder under the load and network conditions before the lower voltage constraint is violated in any hour of the year. (At 15 houses per node, several violations occur in August and September.)

This loading condition means that 168 houses are present on the full feeder. For the five-node feeder variants (Figures 5b and 5c), we assign 33 houses per node (a total of 165) for consistency. Figure 8 shows the voltage (all and average) and LTC operation for 33 houses per feeder for the ‘ near’ and ‘far’ variants. This loading condition

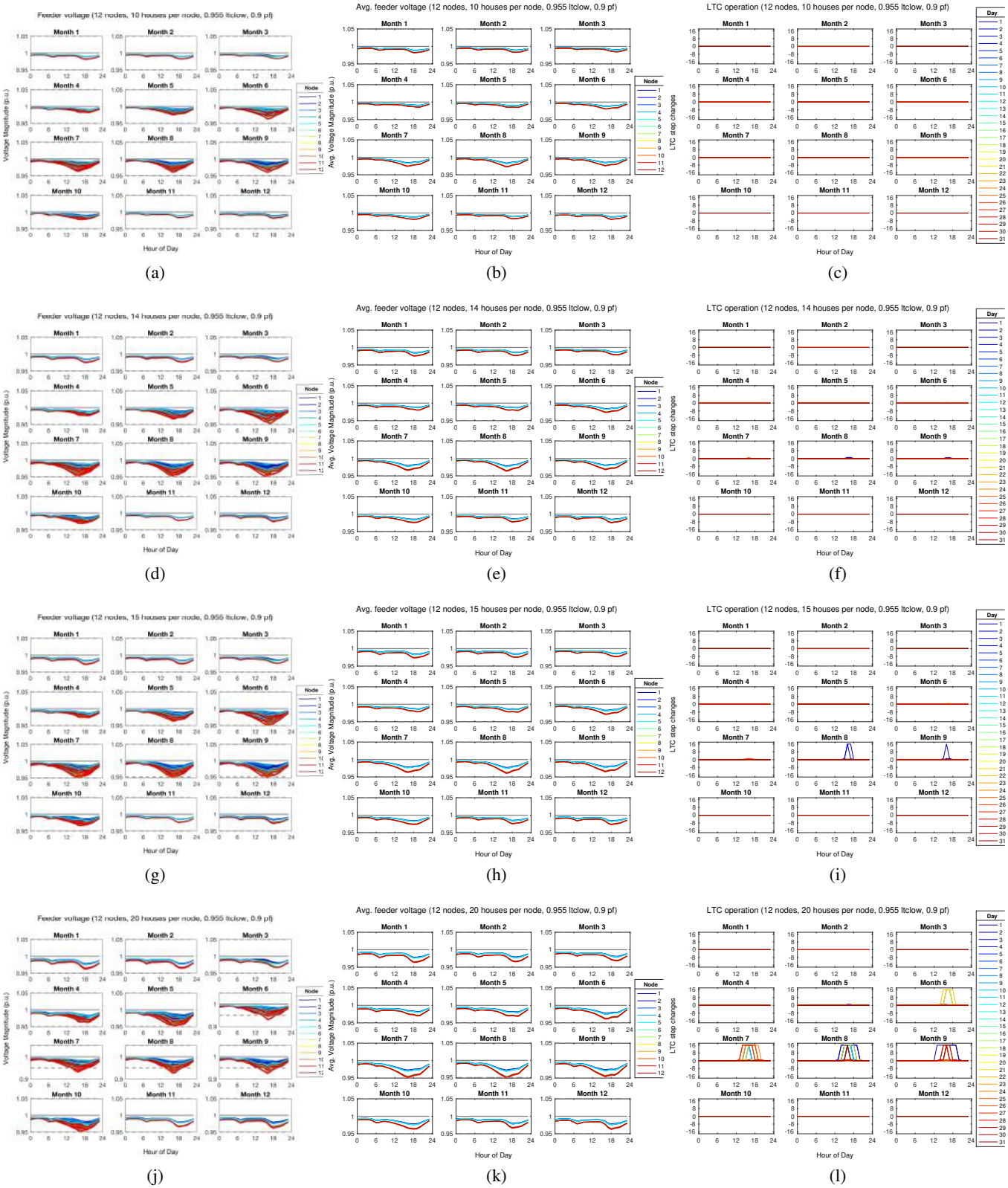

Fig. 7. Feeder voltage at all hours of the year (column 1), at average hours by month (column 2), and LTC operation (column 3) for baseline voltage on the full 12-node feeder when 10 houses (row 1), 14 houses (row 2), 15 houses (row 3), and 20 houses (row 4) are sited per node.

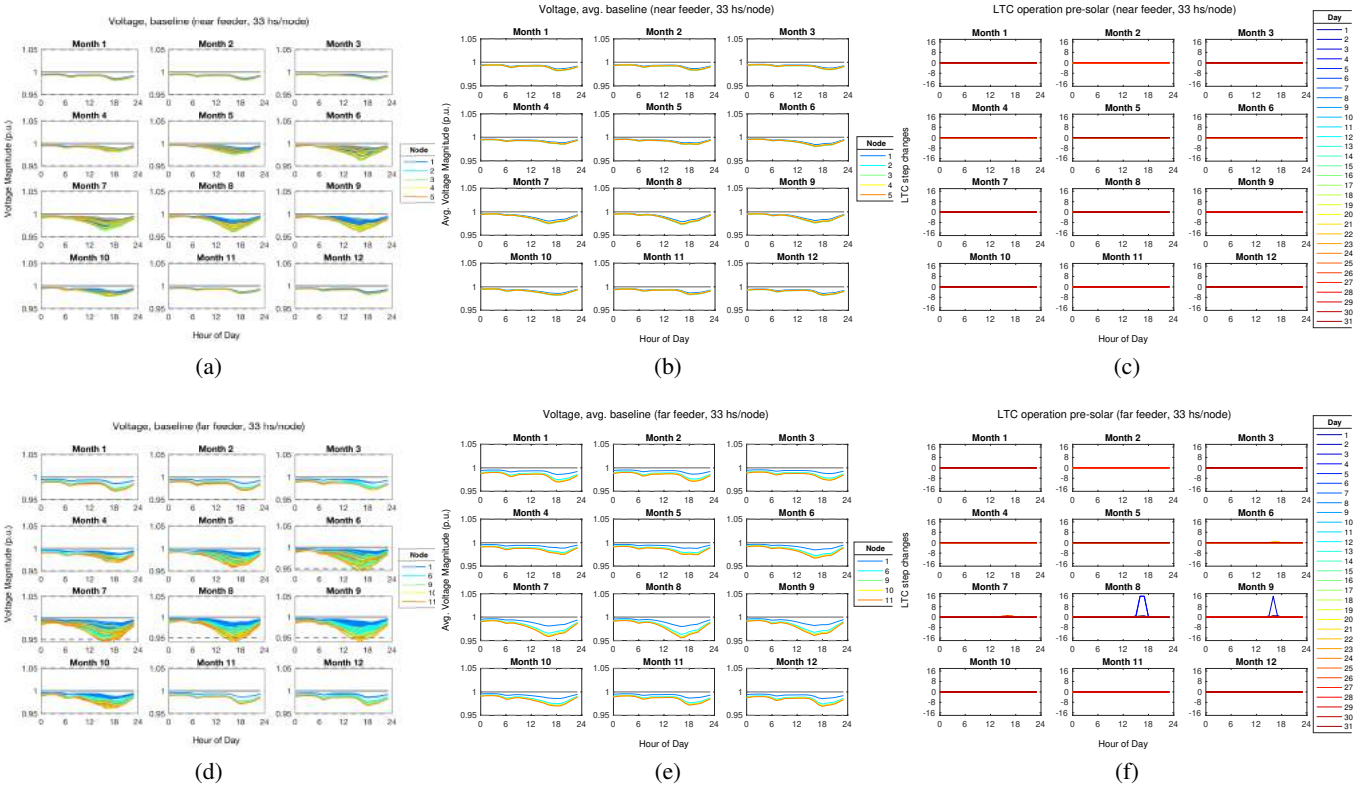

Fig. 8. Feeder voltage at all hours of the year (column 1), at average hours by month (column 2), and LTC operation (column 3) for baseline voltage on the 'near' and 'far' 5-node feeder variants, (rows 1 and 2, respectively) when 33 houses are sited per node.

does not bring the 'near' feeder close to violating its voltage boundaries, but the lower voltage bound is violated by the 'far' feeder for several days in August and September. In the spirit of consistency, we allow this voltage violation and proceed with this loading condition for the 'far' variant. (However, we will remove the lower voltage bound in the optimization to make the problem feasible. In our problem formulation, solar can only raise the voltage on the feeder, so removing this constraint will not affect the amount of solar deployed.)

2) Assigning solar to houses and nodes: We pull hourly production data for 1 kW (residential rooftop) and 100 kW (community) arrays into datasets corresponding to viable tilt/azimuth and mount scenarios. We build up the matrices `P_s_hr` and `P_s_hs` by assigning the hourly production for the selected scenario to each hour and house on the feeder, respectively, and calculate the average hours of production by month (`P_s_hravg`). We build up the matrices `P_s_c` and `P_s_cavg` by assigning hourly production for community solar mount types to each hour of the day and calculating average hour production. Solar production in any hour is a linear function of capacity, so the production from any size array can be obtained via:

$$\text{production } (Wh) = \frac{\text{hourly production } (Wh)}{\text{1 kW array}} \times \text{array capacity } (kW) \tag{12}$$

3) Variables, objective function, and constraints:

a) Residential solar: For the residential solar cases (Table IIA), we seek to maximize the total solar deployed on the feeder, allowing deployment to occur at each node simultaneously. The optimization problem, for n ranging

from 1 to the number of nodes in the feeder variant (Figure 5), is:

$$\min\left[-\sum_{i=1}^{n} C_{\text{res},i}\right] \qquad \text{s.t.} \qquad 0kW \leq C_{\text{res},i}, \tag{13}$$

$$C_{\text{res},i} \leq \sum_{hs=1}^{hs_{node}} \frac{P_{b,hs}}{P_{s,1kW,hs}}, \tag{14}$$

$$0.95^2 p.u. \times V_0 \leq V_0 - 2R\left(P_b - P_{s,1kW}. \times C_{\text{res}}\right) - 2XQ_b \leq 1.05^2 p.u. \times V_0 \tag{15}$$

where C_{res} is a 12×1 vector of total residential solar capacities at each node, $P_{b,hs}$ is the total annual power demand of a given house (watt-hours) and $P_{s,1kW,hs}$ is the total annual solar generation potential of a given house from a 1 kW array (watt-hours per kW of capacity). The fraction in Equation 14 evaluates to the maximum installed solar capacity allowed at a given house, from which production will not exceed power demand over the course of a year. This constraint (Equation 14) is designed to mimic net metering incentives. The summation occurs over all houses at a given node.

b) Community solar: For the community solar cases (Table IIB), we seek to maximize the total solar deployed on a single node of the feeder, considering each node in turn. The optimization problem is:

$$\min\left[-C_{\text{comm}}\right] \qquad \text{s.t.} \qquad 0kW \leq C_{\text{comm}}, \tag{16}$$

$$0.95^2 p.u. \times V_0 \leq V_0 - 2R\left(P_b - C_{\text{vec}} \times C_{\text{comm}} \times P_{sc,1kW}\right) - 2XQ_b \leq 1.05^2 p.u. \times V_0 \tag{17}$$

where C_{comm} is a scalar value of the total community solar capacity for the current node and C_{vec} is a 12×1 vector containing a 1 in the position of the node being evaluated and zeros for all other nodes. This formulation constrains community solar deployment to only occur at the specified node.

c) Residential and community solar: For the combined cases (Table IIC), we seek to maximize the total solar deployed. The optimization problem is:

$$\min\left[\left(-\sum_{i=1}^{n} C_{\text{res},i}\right) - C_{\text{comm}}\right] \qquad \text{s.t.} \qquad 0kW \leq C_{\text{res},i}, \tag{18}$$

$$0kW \leq C_{\text{comm}}, \tag{19}$$

$$C_{\text{res},i} \leq \sum_{hs=1}^{hs_{node}} \frac{P_{b,hs}}{P_{s,1kW,hs}}, \tag{20}$$

$$0.95^2 p.u. \times V_0 \leq V_0 - 2R\left(P_b - P_{s,1kW}. \times C_{\text{res}} - C_{\text{vec}} \times C_{\text{comm}} \times P_{sc,1kW}\right) - 2XQ_b \leq 1.05^2 p.u. \times V_0 \tag{21}$$

This formulation considers each node in turn as an option for community solar deployment, and also allows residential solar deployment to occur at the same time across the full feeder.

4) Optimization scenarios: We calculate installed solar capacity for residential scenario A1, community scenarios B1 and B2, and combined scenarios C1 and C2 (Table II), at all hours of the year and average hours (Section II-A4), for three feeder variants (full feeder, 'near' nodes, and 'far' nodes) (Figure 5).

III. Results and Discussion

A. Residential solar deployment

The residential solar scenarios assessed (all arrays sited at a 30 degree tilt and 180 degree azimuth) allow between 830 and 848 kW of solar capacity to be deployed on the feeder (Table III). In all cases, the amount of solar deployed is restricted by the net metering constraint that total solar production must not exceed total nodal load for the year.

We depict deployed residential solar capacity visually in Figure 9. The first column of figures shows the installed capacity by node for both average hour and all hour scenarios. In both cases, these overlap exactly with the 'allowed capacity' as indicated by the net metering limit for each node. The second column shows the installed capacity by ohmic distance of the relevant node from the feeder head. In all cases, the lines connecting capacity values indicate the radial connectivity of the feeder variant. While the first node on the 'near' and 'far' feeder variants is allocated the most solar, this is an artifact of the random allocation of customer loads (and thereby higher net metering limit) rather than a reflection of network constraints.

The average and all-hour voltage profiles for the residential solar case confirm that no binding upper voltage constraints occur for any feeder variant (Figure 10). Several violations of the lower voltage constraint do occur for the 'far' feeder variant, as discussed in Section II-C1.

As the deployment of residential rooftop solar is limited by its compensation mechanism and not technical limits (at least in the scenarios studied), it is possible that devising new compensation mechanisms for rooftop solar could enable more adoption. New compensation mechanisms could have the added benefit of incentivizing modifications to the deployment model that may make it more attractive to grid planners and operators (e.g., west-facing solar, co-location with storage, reactive power support, etc.).

TABLE III
Residential solar deployment by node across scenarios

	Full feeder (kW)		Near feeder variant (kW)		Far feeder variant (kW)	
Node	Avghrs	Allhrs	Avghrs	Allhrs	Avghrs	Allhrs
1	71.49	71.49	183.53	183.53	183.53	183.53
2	74.12	74.12	148.54	148.54	-	-
3	65.70	65.70	171.95	171.95	-	-
4	71.75	71.75	166.17	166.17	-	-
5	84.12	84.12	160.11	160.11	-	-
6	68.60	68.60	-	-	148.54	148.54
7	74.91	74.91	-	-	-	-
8	53.87	53.87	-	-	-	-
9	74.38	74.38	-	-	171.95	171.95
10	62.55	62.55	-	-	166.17	166.17
11	74.38	74.38	-	-	160.11	160.11
12	71.75	71.75	-	-	-	-
Total	847.62	847.62	830.30	830.30	830.30	830.30

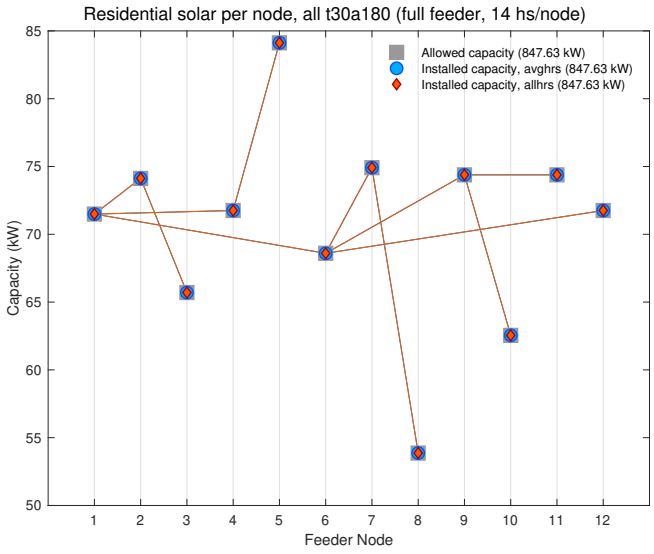

(a)

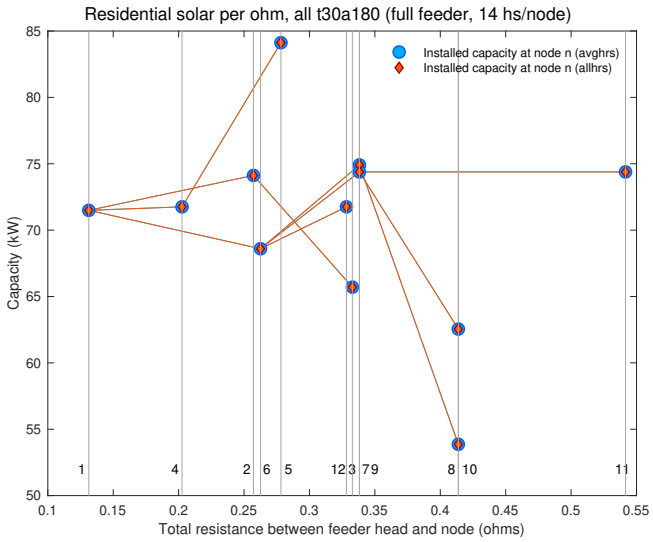

(b)

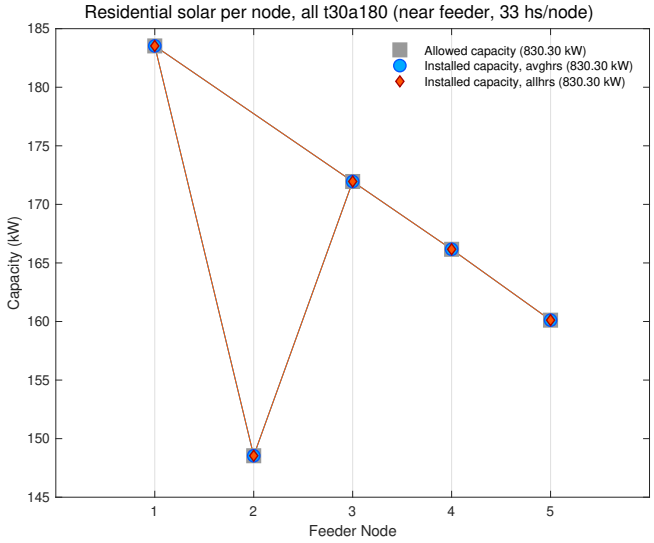

(c)

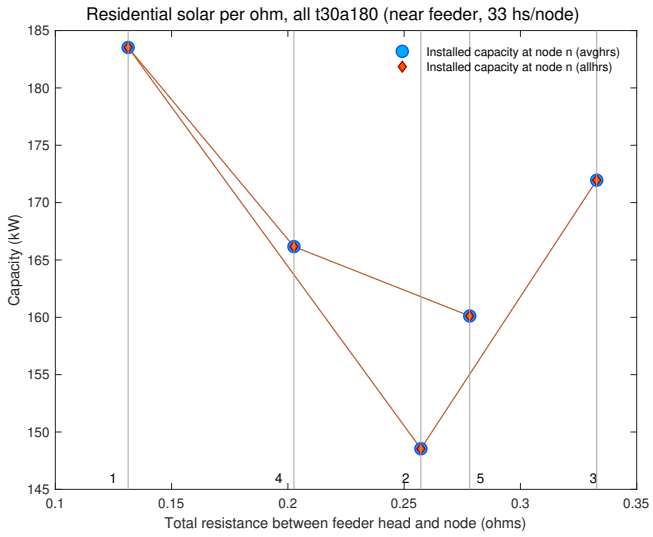

(d)

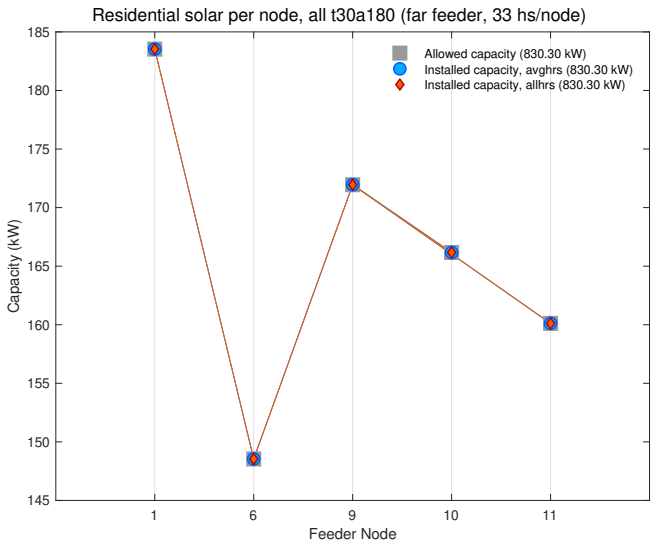

(e)

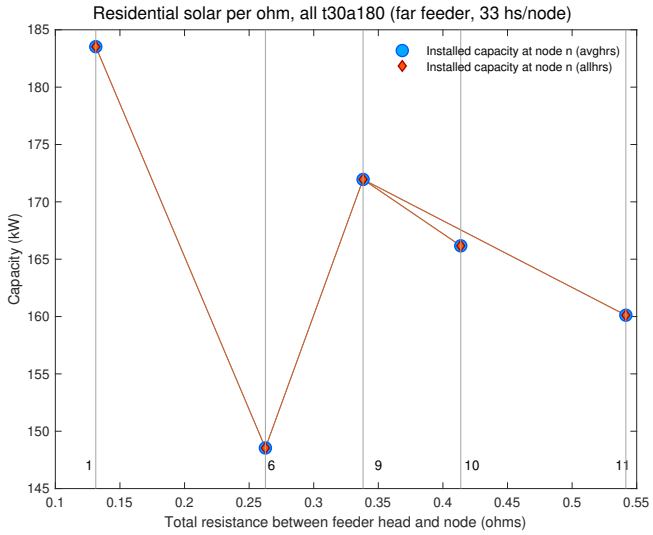

(f)

Fig. 9. Residential solar deployment under fixed tilt/azimuth scenario (all 30 deg. tilt, 180 deg. azimuth) by (a) feeder node and (b) resistance from feeder head under the average hour (blue) and all hour conditions (red).

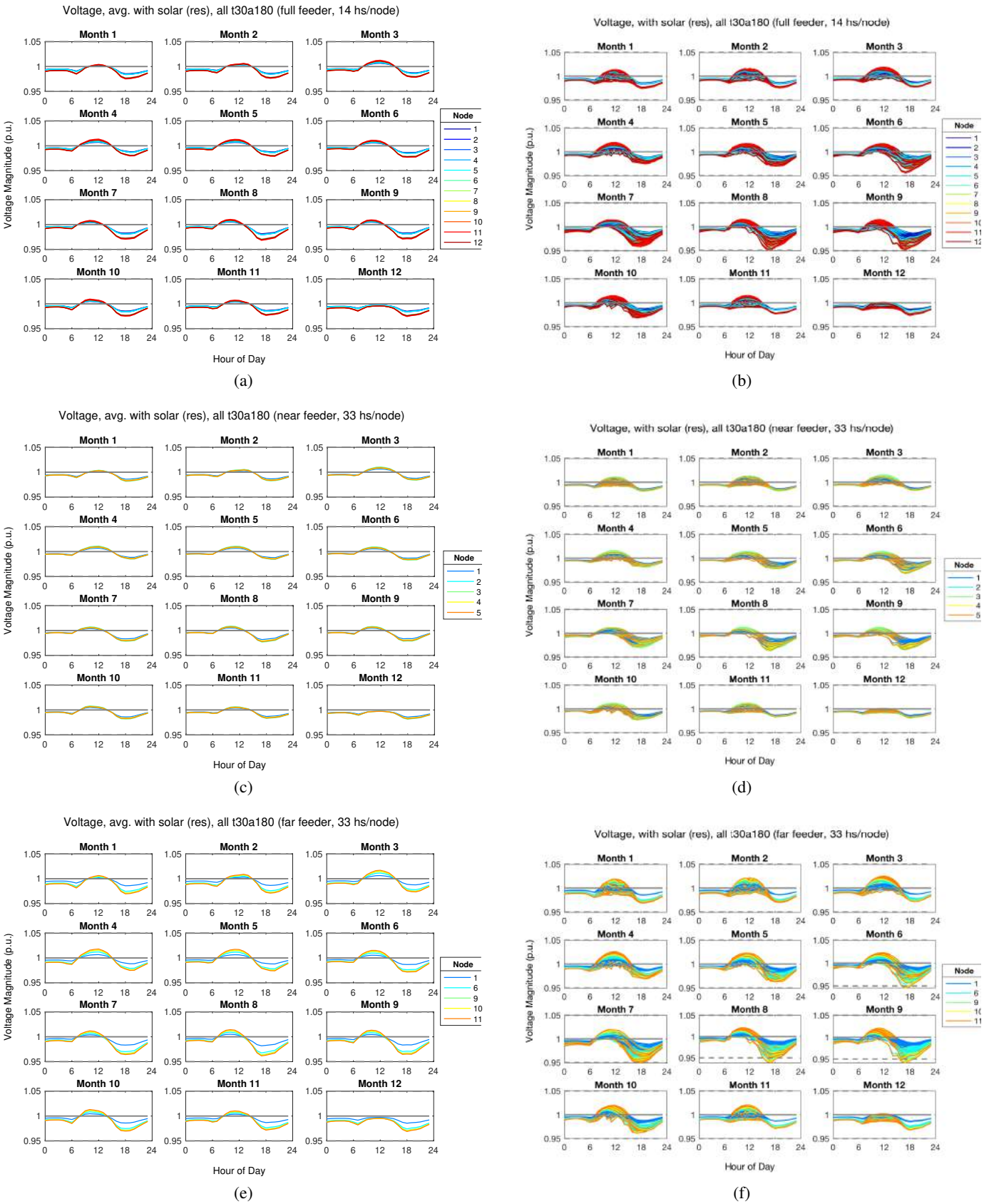

Fig. 10. Feeder voltage following residential solar deployment under the fixed tilt/azimuth scenario (all 30 deg. tilt, 180 deg. azimuth) for the full feeder (row 1), 'near' variant (row 2), and 'far' variant (row 3) for average hours (column 1) and all hours (column 2).

B. Community solar and combined deployment

The community solar scenarios assessed allow between approximately 780 kW and 3.75 MW to be installed on the feeder, depending on the feeder variant and node of installation (Table IV and Figures 11 and 12). As no net metering constraint is present here, the only limitation on solar at a given node is the permissible voltage. For the vast majority of siting decisions (with some exceptions for siting on node 11), significantly more solar capacity can be deployed via community solar over rooftop solar.

Within a mount scenario (fixed vs 1-axis tracking and South- versus Southwest-facing), the allowed capacity numbers are relatively consistent between nodes across feeder variant scenarios (e.g., the first five nodes of the full feeder, and the 'near' feeder variant). Some divergence occurs down the feeder lines, but even nodes 9-11 of the full feeder and 'far' variant allow installed capacities within about 40 kW of each other.

Greater divergence occurs between node indices. Node 1 has the greatest installed capacity for each mount type and feeder scenario, with node 4 coming in second for the full and 'near' variants, and node 6 for the 'far' variant. These are the nodes closest by ohmic distance to the feeder head after node 1. In all cases, allowed capacity declines with ohmic distance from the feeder head, as depicted visually by the shape of the second columns of Figures 11 and 12.

In all cases, less solar is installed in the 'all hour' scenario than the 'average hour' scenario. This is consistent with our intuition that extreme hours may set binding voltage constraints. The difference between these two scenarios may indicate the additional amount of solar capacity that could become available if technologies (e.g., electric vehicles, storage, and demand response and energy efficiency) are adopted and used for hourly and daily smoothing of extreme values.

With few exceptions, the fixed-mount SW-facing scenario has the highest deployment potential across feeder scenarios and node indices. The fixed-mount S-facing scenario is second, though in some places it appears to suffer more from extreme values than the 1-axis tracking S-facing scenario, which is otherwise third. The 1-axis tracking SW-facing scenario has the lowest deployment potential.

Voltage profiles for the fixed-mount and 1-axis tracking scenarios over all hours of the year are shown in Figures 13, 14, 15, and 16 for the full feeder. These figures are meant to depict, by color, overall trends of where voltage limits are reached for each deployment scenario (not intended as a close look at any voltage profile). These limiting nodes are not necessarily the nodes where the solar array is deployed. When community solar is deployed at nodes 1, 2, or 3, the upper voltage limit appears to be reached by one of the first few nodes. For installations at node 4 or 5, the voltage at node 5 appears to contribute the limiting boundary. Deployment at node 6, 9, 10, or 11 means the limit is set by nodes 10 and 11. Deployment at node 7 or 8 means the voltage is set by node 8, and deployment at node 12 means the voltage is set there.

As expected, the highest voltages occur several hours later (around 2 p.m.) for the SW-facing fixed-mount scenario than for its S-facing equivalent. However, the peak for the 1-axis tracking SW-facing scenario is actually shifted earlier than for its S-facing equivalent, which notably has a roughly bimodal distribution in many hours.

TABLE IV
COMMUNITY SOLAR DEPLOYMENT BY NODE ACROSS SCENARIOS

(a) Fixed-mount S-facing (Azimuth 180)

	Full (MW)		Near (MW)		Far (MW)	
Node	Avghrs	Allhrs	Avghrs	Allhrs	Avghrs	Allhrs
1	3.66	2.98	3.65	2.98	3.65	2.98
2	1.89	1.54	1.91	1.55	-	-
3	1.46	1.19	1.49	1.21	-	-
4	2.39	1.95	2.40	1.96	-	-
5	1.75	1.42	1.76	1.44	-	-
6	1.94	1.57	-	-	1.97	1.60
7	1.51	1.23	-	-	-	-
8	1.24	1.00	-	-	-	-
9	1.52	1.23	-	-	1.56	1.26
10	1.24	1.01	-	-	1.29	1.04
11	0.95	0.77	-	-	0.99	0.80
12	1.56	1.26	-	-	-	-
Total*	21.11	17.16	11.21	9.14	9.46	7.68

(b) Fixed-mount SW-facing (Azimuth 225)

	Full (MW)		Near (MW)		Far (MW)	
Node	Avghrs	Allhrs	Avghrs	Allhrs	Avghrs	Allhrs
1	3.75	3.06	3.74	3.05	3.74	3.05
2	1.93	1.58	1.95	1.59	-	-
3	1.50	1.22	1.52	1.24	-	-
4	2.45	1.99	2.46	2.01	-	-
5	1.79	1.46	1.80	1.47	-	-
6	1.98	1.61	-	-	2.02	1.64
7	1.55	1.26	-	-	-	-
8	1.27	1.03	-	-	-	-
9	1.55	1.26	-	-	1.60	1.30
10	1.27	1.03	-	-	1.32	1.07
11	0.98	0.79	-	-	1.01	0.82
12	1.59	1.29	-	-	-	-
Total*	21.61	17.58	11.47	9.36	9.69	7.88

(c) 1-axis tracking S-facing (Azimuth 180)

	Full (MW)		Near (MW)		Far (MW)	
Node	Avghrs	Allhrs	Avghrs	Allhrs	Avghrs	Allhrs
1	3.62	3.23	3.61	3.22	3.61	3.22
2	1.87	1.67	1.89	1.68	-	-
3	1.45	1.29	1.47	1.31	-	-
4	2.36	2.11	2.38	2.12	-	-
5	1.73	1.54	1.74	1.55	-	-
6	1.92	1.71	-	-	1.95	1.73
7	1.50	1.33	-	-	-	-
8	1.22	1.09	-	-	-	-
9	1.50	1.34	-	-	1.54	1.37
10	1.23	1.09	-	-	1.27	1.13
11	0.94	0.84	-	-	0.98	0.86
12	1.54	1.37	-	-	-	-
Total*	20.86	18.60	11.09	9.88	9.35	8.31

(d) 1-axis tracking SW-facing (Azimuth 225)

	Full (MW)		Near (MW)		Far (MW)	
Node	Avghrs	Allhrs	Avghrs	Allhrs	Avghrs	Allhrs
1	3.58	3.00	3.58	3.00	3.58	3.00
2	1.85	1.55	1.87	1.56	-	-
3	1.43	1.20	1.46	1.22	-	-
4	2.34	1.96	2.36	1.97	-	-
5	1.71	1.43	1.73	1.45	-	-
6	1.91	1.59	-	-	1.94	1.61
7	1.49	1.24	-	-	-	-
8	1.22	1.01	-	-	-	-
9	1.50	1.24	-	-	1.54	1.28
10	1.23	1.02	-	-	1.27	1.05
11	0.94	0.78	-	-	0.98	0.81
12	1.53	1.27	-	-	-	-
Total*	20.74	17.30	11.00	9.20	9.31	7.75

*The total values in this table should not be compared directly to the total values in the residential deployment table. In Table III, the totals indicate the full amount of solar that can be deployed on the feeder at once. Here, each *nodal* value is the total amount that can be deployed at once for the given feeder variant and node. The totals here are included here merely as a convenient summary of information for comparison across feeder variants and average vs all hour scenarios.

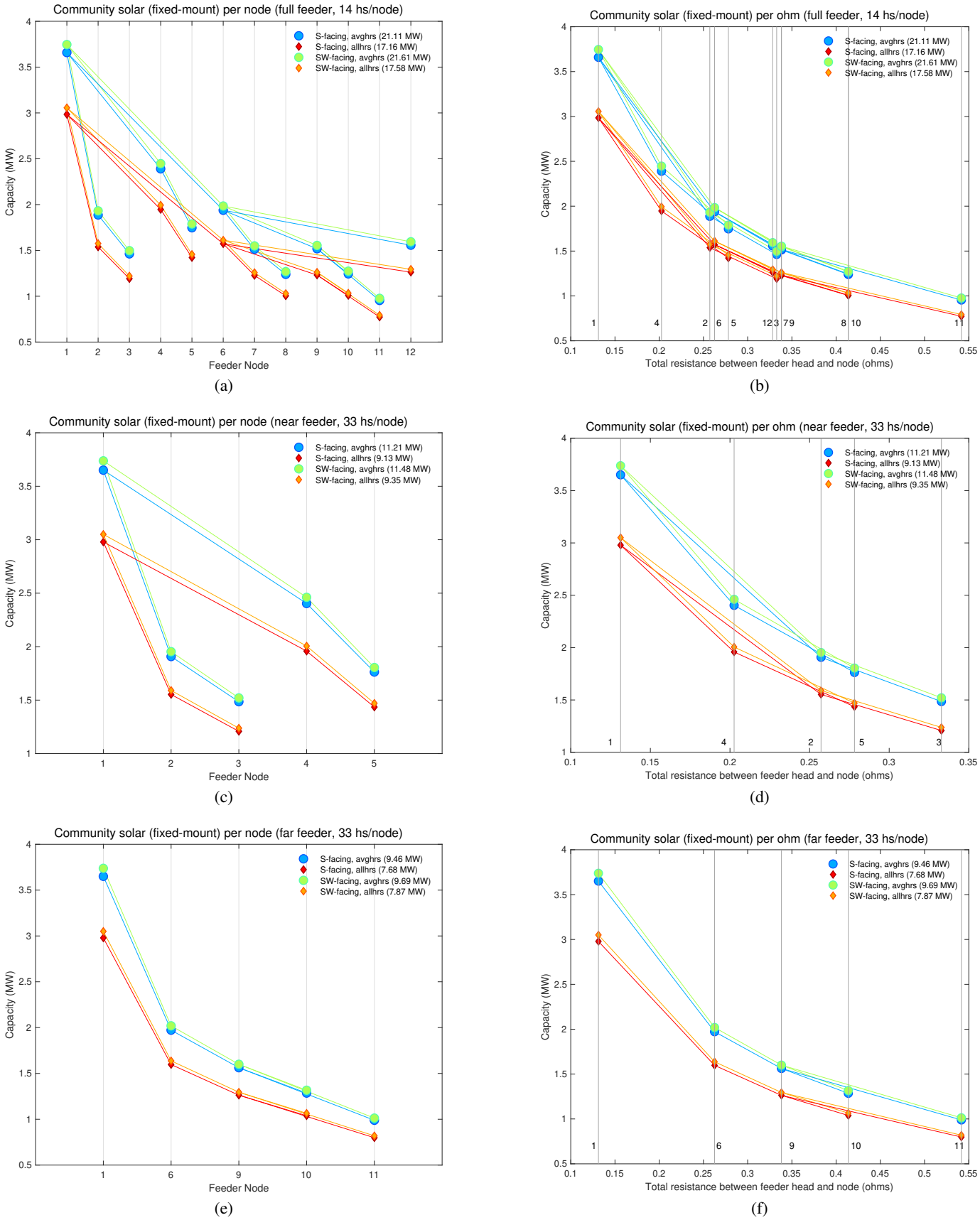

Fig. 11. Community solar deployment for fixed-mount scenarios on the full feeder (row 1), 'near' variant (row 2), and 'far' variant (row 3), shown by feeder node (column 1) and resistance from feeder head (column 2) under the average hour and all hour conditions. Lines indicate radial connections between feeder nodes.

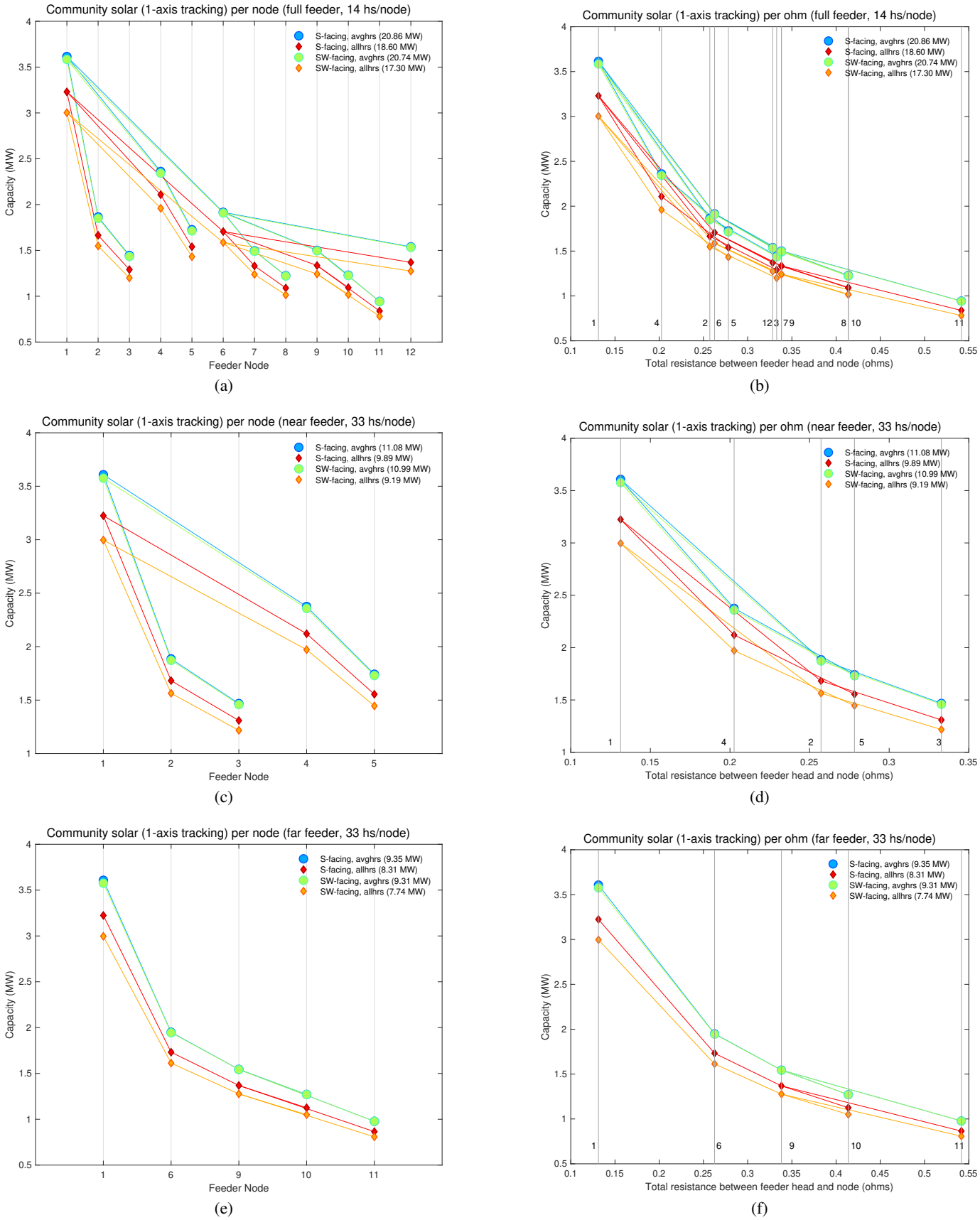

Fig. 12. Community solar deployment for 1-axis backtracking scenarios on the full feeder (row 1), 'near' variant (row 2), and 'far' variant (row 3), shown by feeder node (column 1) and resistance from feeder head (column 2) under the average hour and all hour conditions. Lines indicate radial connections between feeder nodes.

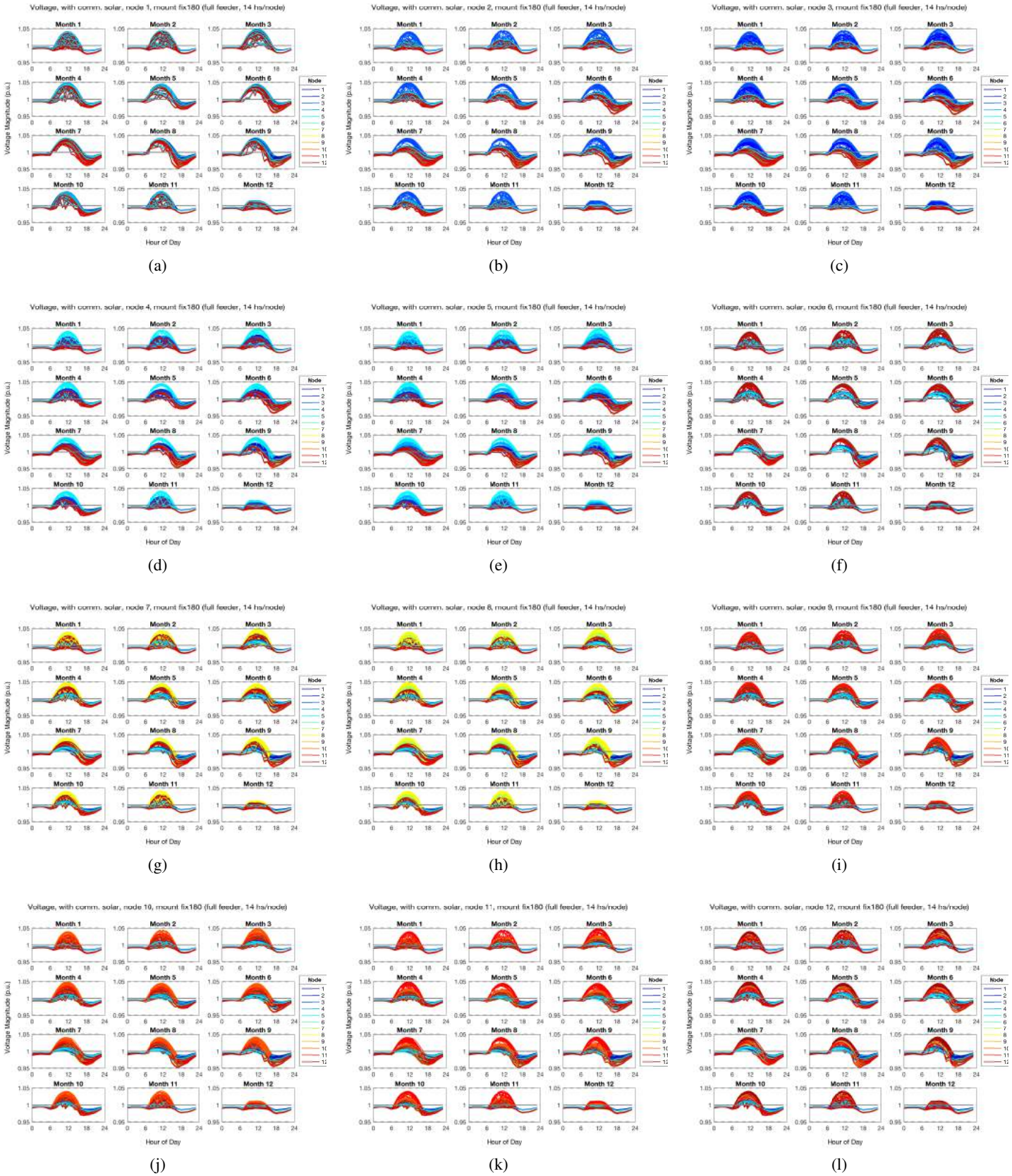

Fig. 13. Feeder voltage following community solar deployment on the full feeder under the fixed-mount S-facing scenario (all 30 deg. tilt, 180 deg. azimuth).

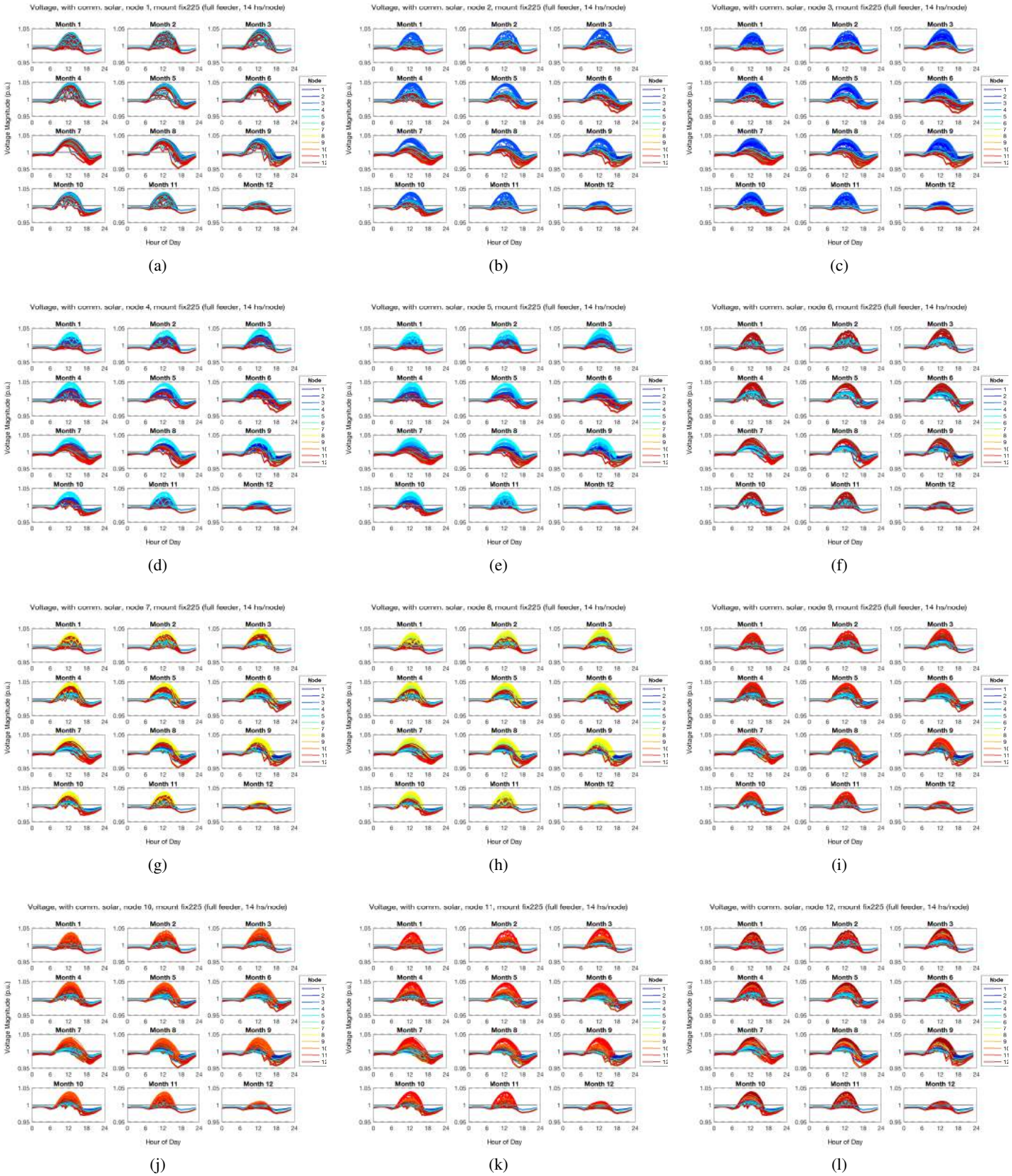

Fig. 14. Feeder voltage following community solar deployment on the full feeder under the fixed-mount SW-facing scenario (all 30 deg. tilt, 225 deg. azimuth).

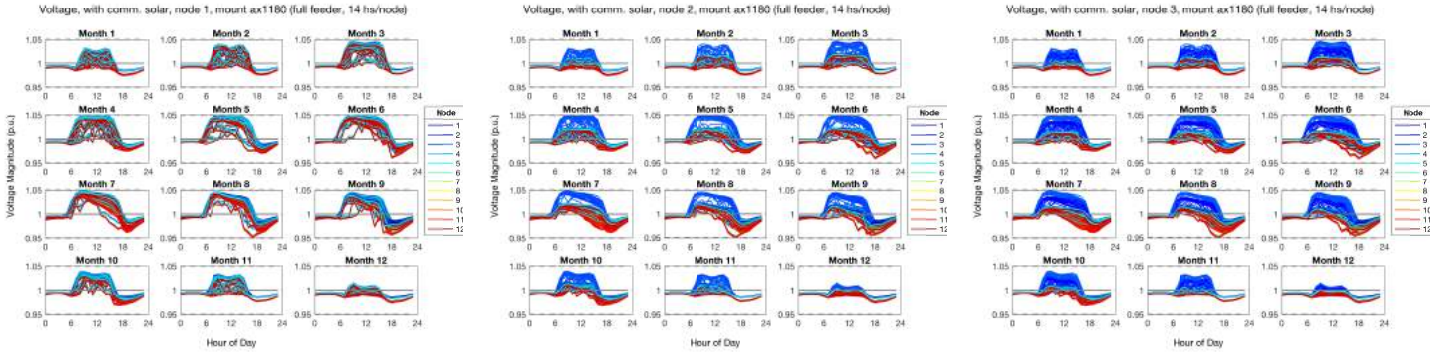

(a)

(b)

(c)

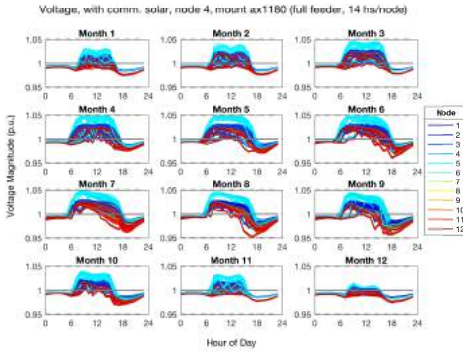

(d)

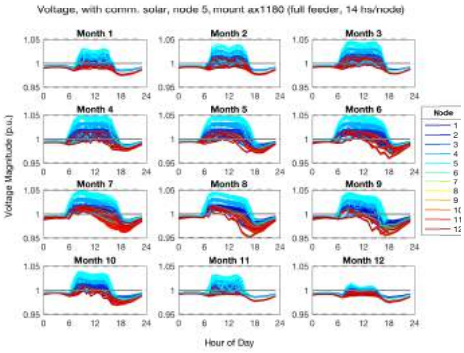

(e)

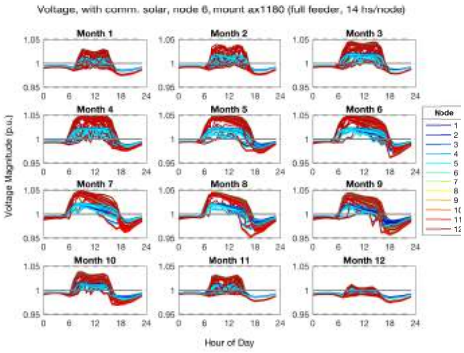

(f)

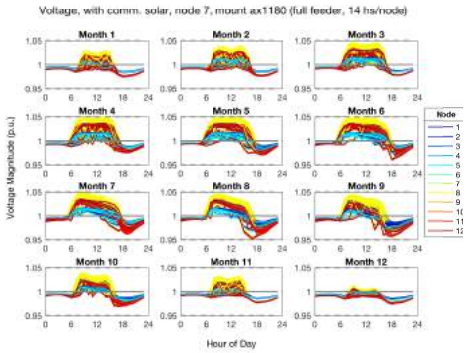

(g)

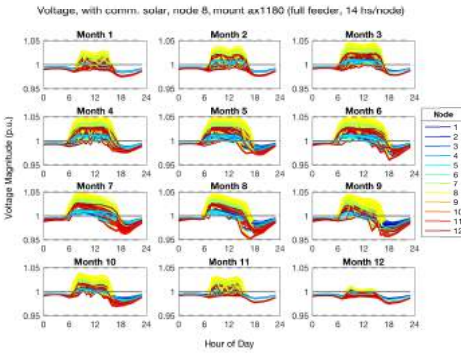

(h)

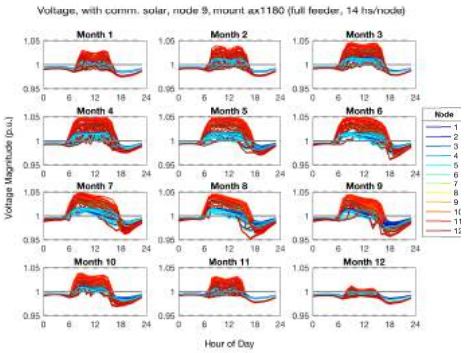

(i)

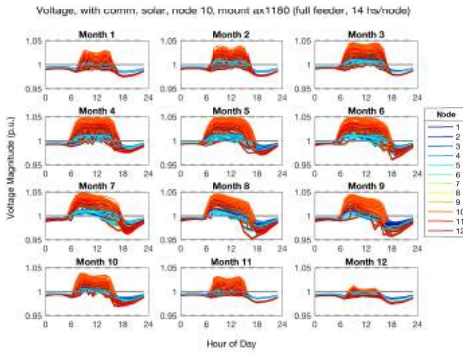

(j)

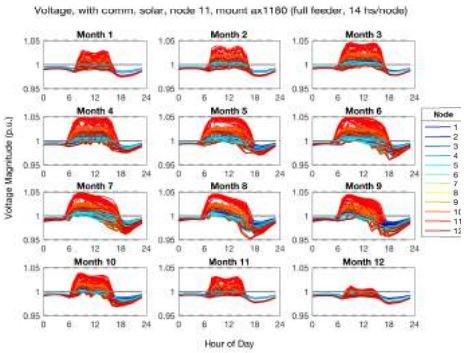

(k)

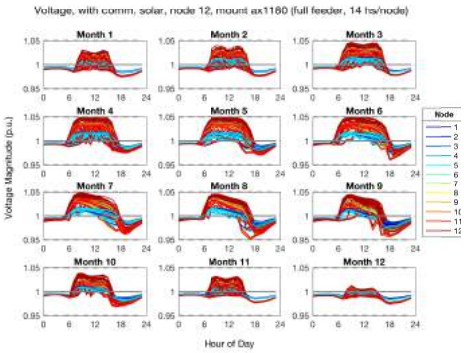

(l)

Fig. 15. Feeder voltage following community solar deployment on the full feeder under the 1-axis tracking S-facing scenario (180 deg. azimuth).

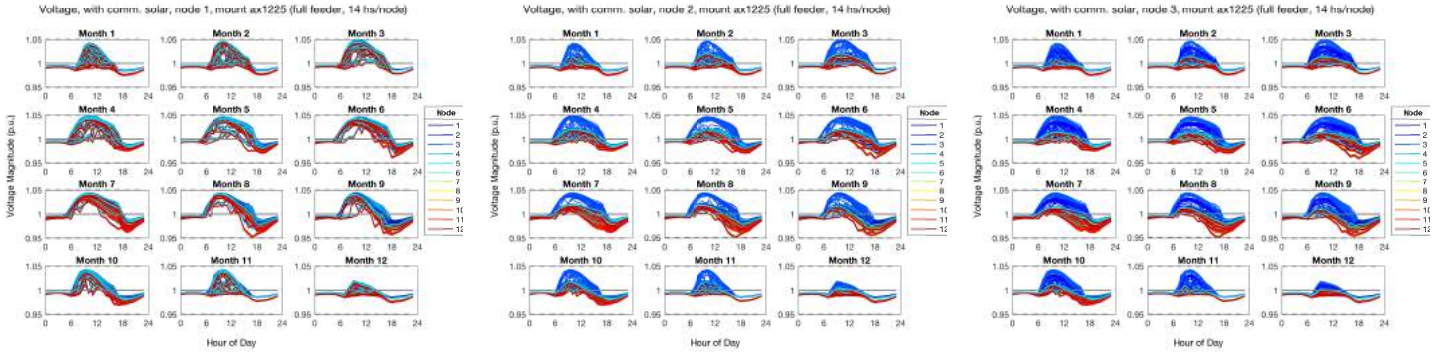

(a)

(b)

(c)

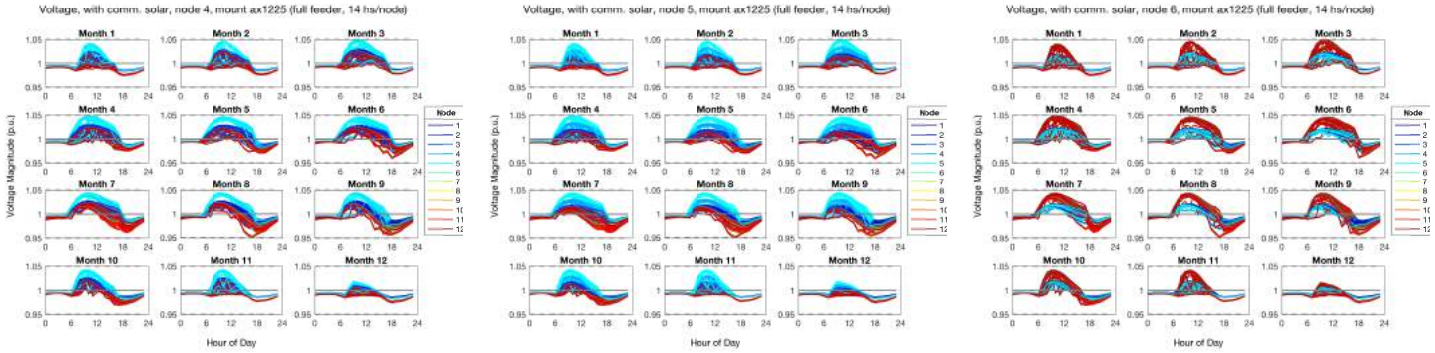

(d)

(e)

(f)

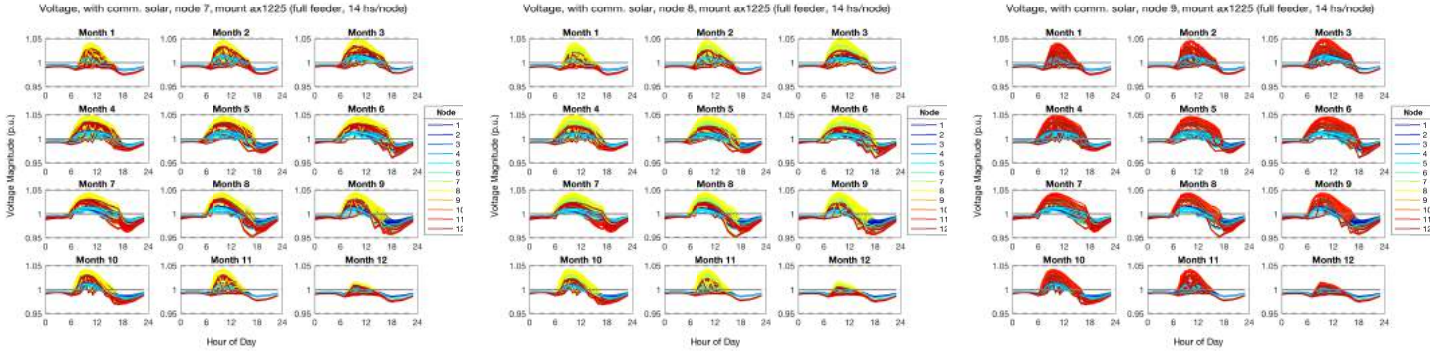

(g)

(h)

(i)

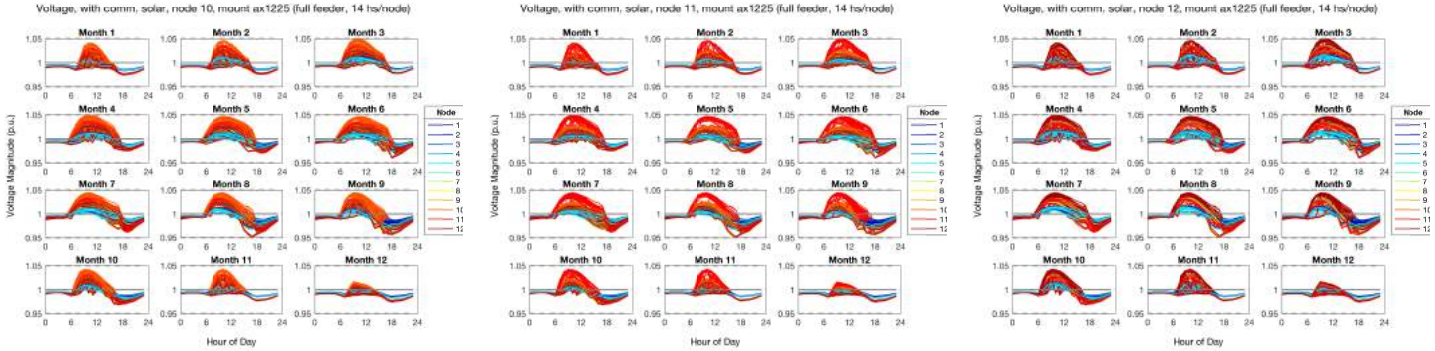

(j)

(k)

(l)

Fig. 16. Feeder voltage following community solar deployment on the full feeder under the 1-axis tracking SW-facing scenario (225 deg. azimuth).

C. Combined deployment

The combined deployment scenarios (C in Table II) allow both residential solar and community solar to be deployed on the feeder at once. In each case, one node is chosen for the community solar location, while residential solar is allowed to be sited on that node as well as every other node on the feeder. Residential solar is still limited by the net metering constraint but community solar is not limited, and the optimization problem solves for the maximum total amount of solar on the feeder (Section II-C3c).

The results for these scenarios are shown in Tables V, VI, and VII for the full, 'near', and 'far' feeder variants, respectively. In all cases, less community solar is deployed on the feeder than in the community-only case for the given mount type and feeder variant. However, more solar is deployed on the feeder overall. The least substantial overall gains are found when community solar is deployed at node 1 (in some cases, barely above rounding error). For any other node chosen, the total amount of solar increases more significantly relative to its community-only comparison case.

This is supported by the pattern of residential deployment that emerges for a given node assigned to the community array. If the community solar is sited at node 1 or node 6, several nodes can no longer accommodate any residential solar. If the community array is located at any other node, every node on the feeder can host residential solar (for many of them, all the way up to their net metering limit).

Yet for all mount types and feeder variants, siting a community solar array at node 1 is still the best choice to achieve the highest overall deployment on the feeder.

TABLE V
FULL FEEDER VARIANT: COMBINED RESIDENTIAL AND COMMUNITY SOLAR DEPLOYMENT BY NODE

(a) Community solar fixed-mount S-facing (azimuth 180)

Comm. location	n01	n01	n02	n02	n03	n03	n04	n04	n05	n05	n06	n06
Timescale	avgh	allh	avgh	allh	avgh	allh	avgh	allh	avgh	allh	avgh	allh
Res. location	resfix	resfix	resfix	resfix	resfix	resfix	resfix	resfix	resfix	resfix	resfix	resfix
n01 (kW)	71.49	71.49	71.49	71.49	71.49	71.49	71.49	71.49	71.49	71.49	71.49	71.49
n02 (kW)	39.46	16.06	74.12	74.12	74.12	74.12	74.12	74.12	74.12	74.12	74.12	74.12
n03 (kW)	0	13.74	18.63	13.74	65.7	65.7	65.7	65.7	65.7	65.7	65.7	65.7
n04 (kW)	54.03	36.71	71.75	71.75	71.75	71.75	71.75	71.75	71.75	71.75	71.75	71.75
n05 (kW)	0	0	84.12	84.12	84.12	84.12	25.11	16.37	84.12	84.12	84.12	84.12
n06 (kW)	68.6	68.6	68.6	68.6	68.6	68.6	68.6	68.6	68.6	68.6	68.6	68.6
n07 (kW)	43.04	26.49	74.91	74.91	74.91	74.91	74.91	74.91	74.91	74.91	36.76	26.49
n08 (kW)	0	0	53.87	53.87	53.87	53.87	53.87	53.87	53.87	53.87	0	0
n09 (kW)	66.06	44.87	74.38	74.38	74.38	74.38	74.38	74.38	74.38	74.38	59.78	44.87
n10 (kW)	0	0	62.55	62.55	62.55	62.55	62.55	62.55	62.55	62.55	0	0
n11 (kW)	0	0	74.38	74.38	74.38	74.38	74.38	74.38	74.38	74.38	0	0
n12 (kW)	40.8	23.35	71.75	71.75	71.75	71.75	71.75	71.75	71.75	71.75	33.58	23.93
CS (kW)	3282.88	2687.61	1441.62	1095.48	1068	795.45	1855.41	1418.49	1293.36	966.3	1563.5	1230.38
Feeder tot. (kW)	3666.35	2988.92	2242.18	1891.15	1915.63	1643.08	2644.03	2198.38	2140.99	1813.93	2129.4	1761.45
Comm. location	n07	n07	n08	n08	n09	n09	n10	n10	n11	n11	n12	n12
Timescale	avgh	allh	avgh	allh	avgh	allh	avgh	allh	avgh	allh	avgh	allh
Res. location	resfix	resfix	resfix	resfix	resfix	resfix	resfix	resfix	resfix	resfix	resfix	resfix
n01 (kW)	71.49	71.49	71.49	71.49	71.49	71.49	71.49	71.49	71.49	71.49	71.49	71.49
n02 (kW)	74.12	74.12	74.12	74.12	74.12	74.12	74.12	74.12	74.12	74.12	74.12	74.12
n03 (kW)	65.7	65.7	65.7	65.7	65.7	65.7	65.7	65.7	65.7	65.7	65.7	65.7
n04 (kW)	71.75	71.75	71.75	71.75	71.75	71.75	71.75	71.75	71.75	71.75	71.75	71.75
n05 (kW)	84.12	84.12	84.12	84.12	84.12	84.12	84.12	84.12	84.12	84.12	84.12	84.12
n06 (kW)	68.6	68.6	68.6	68.6	68.6	68.6	68.6	68.6	68.6	68.6	68.6	68.6
n07 (kW)	74.91	74.91	74.91	74.91	74.91	74.91	74.91	74.91	74.91	74.91	74.91	74.91
n08 (kW)	12.7	9.75	53.87	53.87	53.87	53.87	53.87	53.87	53.87	53.87	53.87	53.87
n09 (kW)	74.38	74.38	74.38	74.38	74.38	74.38	74.38	74.38	74.38	74.38	74.38	74.38
n10 (kW)	62.55	62.55	62.55	62.55	17.98	13.83	62.55	62.55	62.55	62.55	62.55	62.55
n11 (kW)	74.38	74.38	74.38	74.38	16.87	12.53	74.38	74.38	74.38	74.38	74.38	74.38
n12 (kW)	71.75	71.75	71.75	71.75	71.75	71.75	71.75	71.75	71.75	71.75	71.75	71.75
CS (kW)	1019.77	734.2	793.11	556.61	1066.44	785.51	781.84	544.24	582.28	399.64	1022.23	725.35
Feeder tot. (kW)	1826.23	1537.71	1640.74	1404.25	1811.98	1522.58	1629.47	1391.87	1429.91	1247.27	1869.86	1572.98

(b) Community solar 1-axis tracking SW-facing (azimuth 225)

Comm. location	n01	n01	n02	n02	n03	n03	n04	n04	n05	n05	n06	n06
Timescale	avgh	allh	avgh	allh	avgh	allh	avgh	allh	avgh	allh	avgh	allh
Res. location	resfix	resfix	resfix	resfix	resfix	resfix	resfix	resfix	resfix	resfix	resfix	resfix
n01 (kW)	71.49	71.49	71.49	71.49	71.49	71.49	71.49	71.49	71.49	71.49	71.49	71.49
n02 (kW)	46.54	34.45	74.12	74.12	74.12	74.12	74.12	74.12	74.12	74.12	74.12	74.12
n03 (kW)	0	0	21.53	14.24	65.7	65.7	65.7	65.7	65.7	65.7	65.7	65.7
n04 (kW)	62.01	42.66	71.75	71.75	71.75	71.75	71.75	71.75	71.75	71.75	71.75	71.75
n05 (kW)	0	0	84.12	84.12	84.12	84.12	28.65	17.17	84.12	84.12	84.12	84.12
n06 (kW)	68.6	68.6	68.6	68.6	68.6	68.6	68.6	68.6	68.6	68.6	68.6	68.6
n07 (kW)	52.26	32.89	74.91	74.91	74.91	74.91	74.91	74.91	74.91	74.91	70.55	27.39
n08 (kW)	0	0	53.87	53.87	53.87	53.87	53.87	53.87	53.87	53.87	0	0
n09 (kW)	74.38	54.5	74.38	74.38	74.38	74.38	74.38	74.38	74.38	74.38	74.38	46.72
n10 (kW)	6.36	0	62.55	62.55	62.55	62.55	62.55	62.55	62.55	62.55	4.7	0
n11 (kW)	0	0	74.38	74.38	74.38	74.38	74.38	74.38	74.38	74.38	19.95	0
n12 (kW)	50.7	30.66	71.75	71.75	71.75	71.75	71.75	71.75	71.75	71.75	71.75	24.91
CS (kW)	3194.78	2698.26	1438.82	1127.77	1072.23	820.43	1848.47	1459.41	1296.24	996.27	1456.58	1262.82
Feeder tot. (kW)	3627.12	3033.51	2242.28	1923.94	1919.86	1668.06	2640.63	2240.09	2143.87	1843.9	2133.71	1797.63
Comm. location	n07	n07	n08	n08	n09	n09	n10	n10	n11	n11	n12	n12
Timescale	avgh	allh	avgh	allh	avgh	allh	avgh	allh	avgh	allh	avgh	allh
Res. location	resfix	resfix	resfix	resfix	resfix	resfix	resfix	resfix	resfix	resfix	resfix	resfix
n01 (kW)	71.49	71.49	71.49	71.49	71.49	71.49	71.49	71.49	71.49	71.49	71.49	71.49
n02 (kW)	74.12	74.12	74.12	74.12	74.12	74.12	74.12	74.12	74.12	74.12	74.12	74.12
n03 (kW)	65.7	65.7	65.7	65.7	65.7	65.7	65.7	65.7	65.7	65.7	65.7	65.7
n04 (kW)	71.75	71.75	71.75	71.75	71.75	71.75	71.75	71.75	71.75	71.75	71.75	71.75
n05 (kW)	84.12	84.12	84.12	84.12	84.12	84.12	84.12	84.12	84.12	84.12	84.12	84.12
n06 (kW)	68.6	68.6	68.6	68.6	68.6	68.6	68.6	68.6	68.6	68.6	68.6	68.6
n07 (kW)	74.91	74.91	74.91	74.91	74.91	74.91	74.91	74.91	74.91	74.91	74.91	74.91
n08 (kW)	14.35	9.97	53.87	53.87	53.87	53.87	53.87	53.87	53.87	53.87	53.87	53.87
n09 (kW)	74.38	74.38	74.38	74.38	74.38	74.38	74.38	74.38	74.38	74.38	74.38	74.38
n10 (kW)	62.55	62.55	62.55	62.55	20.97	14.3	62.55	62.55	62.55	62.55	62.55	62.55
n11 (kW)	74.38	74.38	74.38	74.38	19.95	13.09	74.38	74.38	74.38	74.38	74.38	74.38
n12 (kW)	71.75	71.75	71.75	71.75	71.75	71.75	71.75	71.75	71.75	71.75	71.75	71.75
CS (kW)	1035.7	760.21	810.93	577.68	1075.67	811.41	801.7	565.41	599.35	415.81	1042.37	752.06
Feeder tot. (kW)	1843.82	1563.94	1658.56	1425.31	1827.29	1549.5	1649.33	1413.04	1446.99	1263.44	1890	1599.7

TABLE VI
NEAR FEEDER VARIANT: COMBINED RESIDENTIAL AND COMMUNITY SOLAR DEPLOYMENT BY NODE

(a) Community solar fixed-mount S-facing (azimuth 180)										
Comm. location	n01	n01	n02	n02	n03	n03	n04	n04	n05	n05
Timescale	avgh	allh	avgh	allh	avgh	allh	avgh	allh	avgh	allh
Res. location	resfix	resfix	resfix	resfix	resfix	resfix	resfix	resfix	resfix	resfix
n01 (kW)	183.53	183.53	183.53	183.53	183.53	183.53	183.53	183.53	183.53	183.53
n02 (kW)	91.41	66.64	148.54	148.54	148.54	148.54	148.54	148.54	148.54	148.54
n03 (kW)	0	0	49.26	35.79	171.95	171.95	171.95	171.95	171.95	171.95
n04 (kW)	109.88	80.2	166.17	166.17	166.17	166.17	166.17	166.17	166.17	166.17
n05 (kW)	0	0	160.11	160.11	160.11	160.11	45.53	33.48	160.11	160.11
CS (kW)	3273.44	2653.46	1458.51	1114.95	1006.93	727.57	1876.11	1439.97	1253.96	923.95
Feeder total (kW)	3658.26	2983.82	2166.12	1809.09	1837.23	1557.87	2591.82	2143.64	2084.27	1754.25
(b) Community solar 1-axis tracking SW-facing (azimuth 225)										
Comm. location	n01	n01	n02	n02	n03	n03	n04	n04	n05	n05
Timescale	avgh	allh	avgh	allh	avgh	allh	avgh	allh	avgh	allh
Res. location	resfix	resfix	resfix	resfix	resfix	resfix	resfix	resfix	resfix	resfix
n01 (kW)	183.53	183.53	183.53	183.53	183.53	183.53	183.53	183.53	183.53	183.53
n02 (kW)	105.73	76.66	148.54	148.54	148.54	148.54	148.54	148.54	148.54	148.54
n03 (kW)	0	0	57.54	37.32	171.95	171.95	171.95	171.95	171.95	171.95
n04 (kW)	127.53	92.44	166.17	166.17	166.17	166.17	166.17	166.17	166.17	166.17
n05 (kW)	0	0	160.11	160.11	160.11	160.11	52.85	34.76	160.11	160.11
CS (kW)	3200.17	2676.52	1452.09	1146.9	1019.28	752.54	1866.4	1480.95	1262.69	953.91
Feeder total (kW)	3616.97	3029.15	2167.98	1842.57	1849.58	1582.84	2589.43	2185.9	2092.99	1784.21

TABLE VII
FAR FEEDER VARIANT: COMBINED RESIDENTIAL AND COMMUNITY SOLAR DEPLOYMENT BY NODE

(a) Community solar fixed-mount S-facing (azimuth 180)										
Comm. location	n01	n01	n06	n06	n09	n09	n10	n10	n11	n11
Timescale	avgh	allh	avgh	allh	avgh	allh	avgh	allh	avgh	allh
Res. location	resfix	resfix	resfix	resfix	resfix	resfix	resfix	resfix	resfix	resfix
n01 (kW)	183.53	183.53	183.53	183.53	183.53	183.53	183.53	183.53	183.53	183.53
n06 (kW)	148.54	148.54	148.54	148.54	148.54	148.54	148.54	148.54	148.54	148.54
n09 (kW)	148.01	70.15	142.36	103.74	171.95	171.95	171.95	171.95	171.95	171.95
n10 (kW)	0	0	0	0	49.04	35.54	166.17	166.17	166.17	166.17
n11 (kW)	0	0	0	0	36.29	26.69	160.11	160.11	160.11	160.11
CS (kW)	3180.07	2582.7	1597.17	1258.26	1127.49	848.53	707.5	457.45	510.99	318.12
Feeder total (kW)	3660.14	2984.91	2071.59	1694.07	1716.84	1414.78	1537.8	1287.75	1341.29	1148.42
(b) Community solar 1-axis tracking SW-facing (azimuth 225)										
Comm. location	n01	n01	n06	n06	n09	n09	n10	n10	n11	n11
Timescale	avgh	allh	avgh	allh	avgh	allh	avgh	allh	avgh	allh
Res. location	resfix	resfix	resfix	resfix	resfix	resfix	resfix	resfix	resfix	resfix
n01 (kW)	183.53	183.53	183.53	183.53	183.53	183.53	183.53	183.53	183.53	183.53
n06 (kW)	148.54	148.54	148.54	148.54	148.54	148.54	148.54	148.54	148.54	148.54
n09 (kW)	171.95	94.65	165.6	107.94	171.95	171.95	171.95	171.95	171.95	171.95
n10 (kW)	14.74	0	0	0	56.92	36.97	166.17	166.17	166.17	166.17
n11 (kW)	0	0	0	0	42.12	27.71	160.11	160.11	160.11	160.11
CS (kW)	3108.42	2609.26	1578.65	1291.41	1130.94	874.82	738.13	479	534.85	334.47
Feeder total (kW)	3627.18	3035.97	2076.32	1731.42	1733.99	1443.52	1568.43	1309.3	1365.16	1164.77

D. Total solar deployment

We compare all cases (residential-only, community-only, and combined) with respect to the total amount of solar they are able to deploy on each of the feeder variants (Figures 17 and 18). We note that the difference between average hours and all hours of evaluation, as well as the difference between the community solar array and the residential contribution, dwarfs the difference between the two mount types. In this comparison, we see that the contribution of residential solar can be substantial, and allowing residential solar deployment in concert with a community array can significantly boost the overall solar present on the feeder.

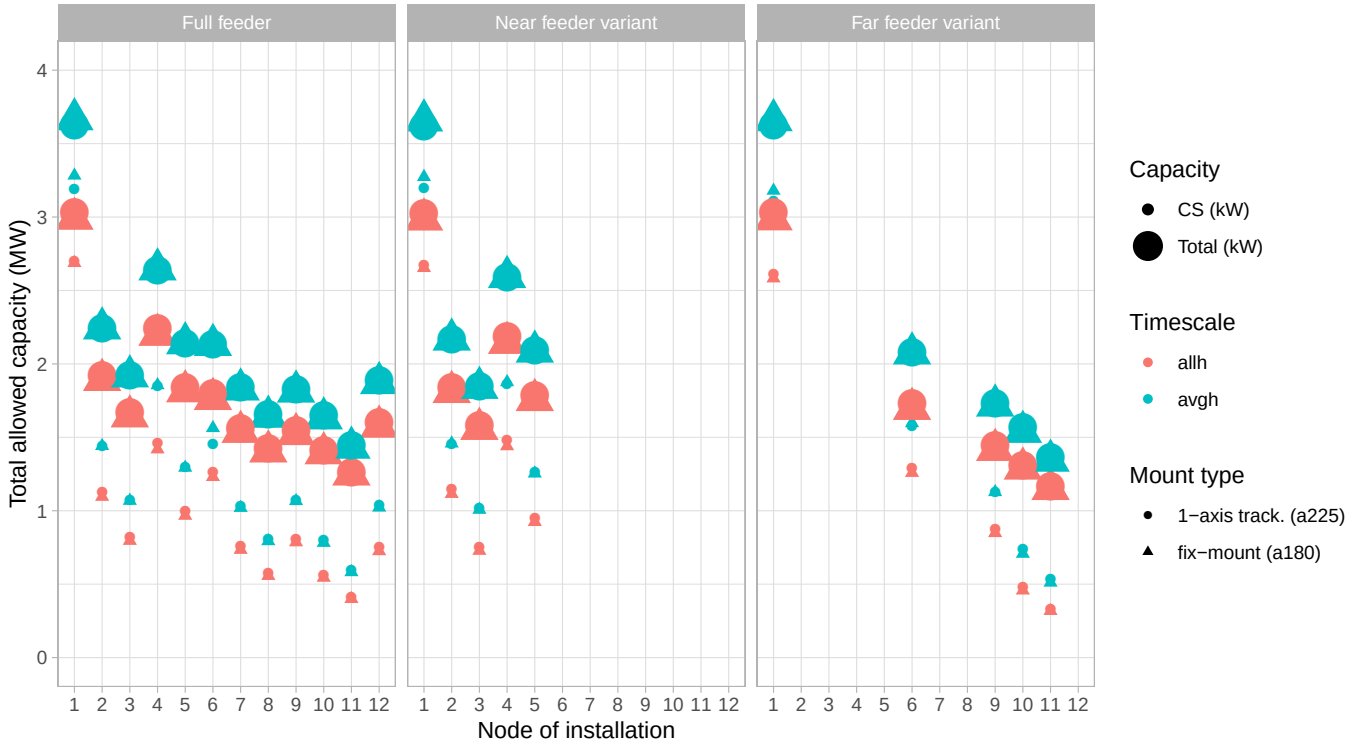

Fig. 17. Total solar allowed on network under combined residential and community scenarios for fixed-mount S-facing and 1-axis tracking SW-facing mounts. Small markers show the contribution of community solar to each combined scenario, while larger markers show the total solar deployment under that scenario. The difference between small and large markers, therefore, is the contribution that residential solar makes to the overall solar capacity. Where only a triangle is shown, the circle overlaps with it entirely.

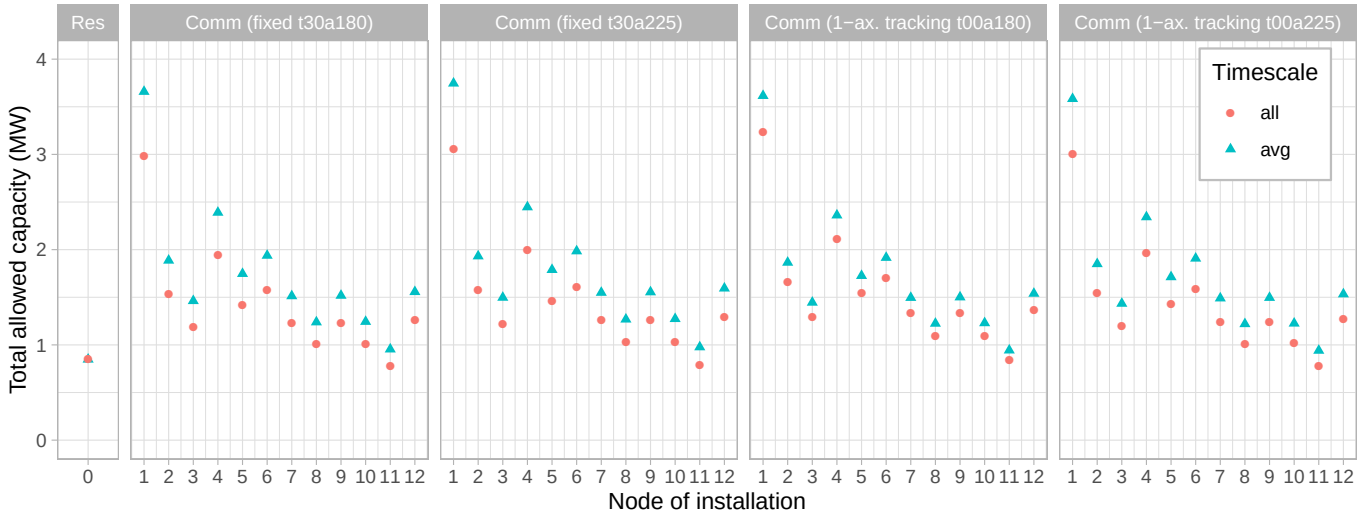

(a)

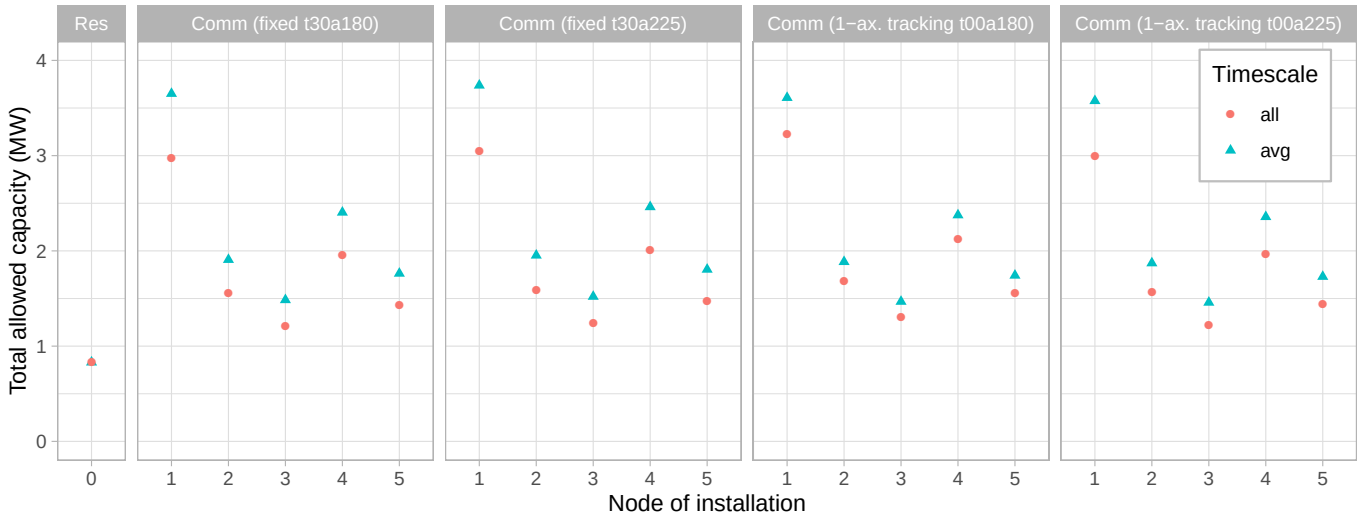

(b)

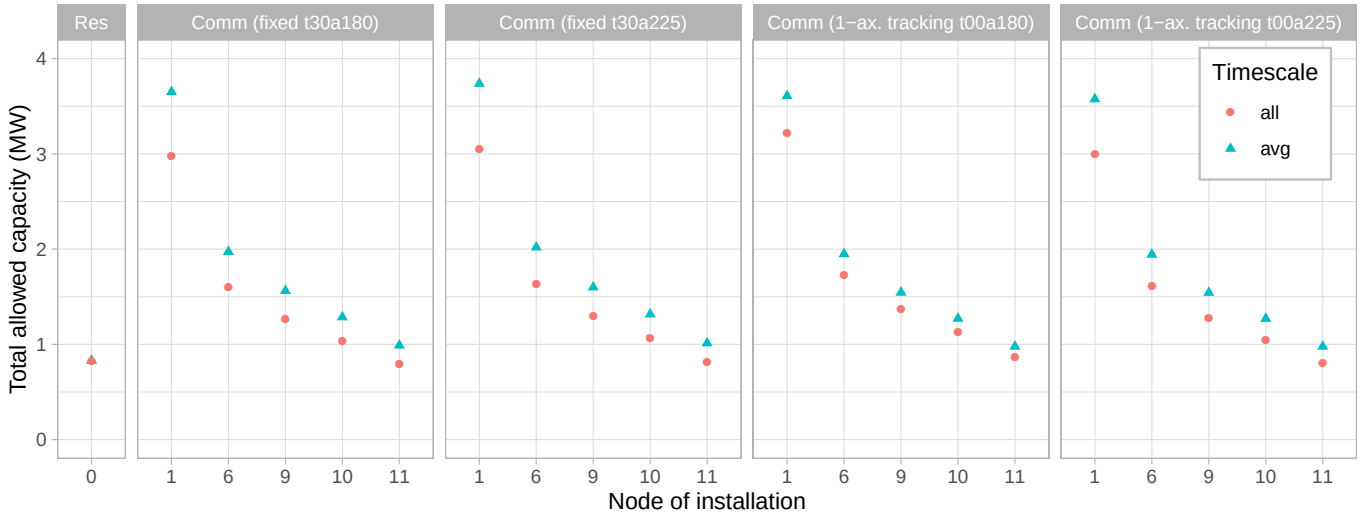

(c)

Fig. 18. Total solar allowed on network under residential and community scenarios for (a) full feeder, (b) 'near' variant, and (c) 'far' variant. In the residential solar scenario, the the total allowed capacity is summed across all nodes in the feeder. In the community solar scenarios, the total allowed capacity is calculated per node, with all other nodes set to 0.

IV. Conclusions and Future Work

The physical and policy-relevant characteristics of residential rooftop solar and community solar impact the deployment potential of these two business models. Specifically, we find that, in the scenarios studied, residential rooftop solar is limited not by voltage bounds but rather by the net metering compensation mechanism it is subject to. By contrast, community solar is limited by the allowable voltage bounds on a particular feeder. In the combined scenarios, pairing community solar with residential rooftop solar enables increased deployment throughout the feeder. We find that the highest possible capacity of solar does not change significantly between the community solar and combined (community and residential) cases. However, allowing both deployment models does substantially increase potential deployment if community solar is sited beyond the node closest to the substation. While community solar allows greater siting flexibility than residential rooftop, it may not always be possible to site arrays at the chosen node in real-world deployment scenarios.

We confirm our initial hypothesis that evaluating all hours over the chosen year rather than average hours by month substantially reduces the allowable deployment capacity. We posit that the difference in allowable capacity between these two scenarios may illuminate the potential for additional solar deployment if other technologies (e.g., electric vehicles, storage, and energy efficiency and demand response) are used to smooth hourly and daily extremes.

Of the three feeder variants studied, the full feeder can host significantly more community and combined community-and-residential capacity than its ‘near’ and ‘far’ variants. (The three are similar in the residential-only case, as all are limited by net metering constraints.) This is consistent with our observation that allowable capacity declines with ohmic distance from the substation. The network structure is key to understanding solar deployment potential, and we will consider more realistic (and larger) feeder scenarios in future work.

The present discussion omits analysis of the impact of resistive losses, reactive power support by inverters, and the potential for load tap changers and other voltage regulating devices to step down voltage during hours of high solar production. We also neglect to perform an analysis of the implications of climate via varying geographic scenarios for load and solar irradiance, assess the real-world mix of residential panel tilt and orientations, or to evaluate the implications for total energy production as well as installed capacity. We will return to these topics in future work.

Acknowledgments

I am grateful to Mingxi Liu for help formulating the problem setup and members of the Energy Modeling, Control, and Analysis research group for early feedback on the project and its scope. Phillippe Phanivong and Antoine Lesage-Landry kindly helped trouble-shoot aspects of the methodology and analysis. I am grateful to my readers, Duncan Callaway and Kameshwar Poolla, for engaging thoughtfully with this work and providing valuable feedback.

APPENDIX A
POWER FLOW EQUATIONS FOR A SINGLE-PHASE RADIAL DISTRIBUTION FEEDER

We formulate the optimization problem with reference to power flow equations applied to a single-phase radial distribution feeder. The following power flow variables are defined at each node i of the network:

TABLE VIII
POWER FLOW VARIABLES

Injected to node i	P_i	Real power
	Q_i	Reactive power
	S_i	Complex power
	I_i	Current
Consumed by load located at the node i	p_i	Real power
	q_i	Reactive power
	s_i	Complex power
	i_i	Current
Experienced at node i	V_i	Voltage
Between node i and downstream node j	r_{ij}	Resistance
	x_{ij}	Reactance
	Z_{ij}	Impedance

Complex power is defined as:

$$S_i = V_i I_i^* = P_i + jQ_i \tag{22}$$

The line impedance between nodes i and j can be written as a complex number:

$$Z_{ij} = r_{ij} + jx_{ij} \tag{23}$$

At each node i, we can represent the current and voltage in terms of the current and voltage experienced by the downstream nodes with reference to Kirchhoff's Laws:

$$I_i = i_i + \sum_j I_j \tag{24}$$

$$V_i = V_j + Z_{ij} I_j \tag{25}$$

Combining the above equations, we can write complex power at node i as:

$$\begin{aligned}
S_i &= V_i I_i^* \\
&= V_i \left(i_i + \sum_j I_j \right)^* \\
&= V_i i_i^* + V_i \sum_j I_j^* \\
&= V_i i_i^* + \sum_j V_i I_j^* \\
&= V_i i_i^* + \sum_j \left(V_j + Z_{ij} I_j \right) I_j^* \\
&= s_i + \sum_j V_j I_j^* + \sum_j Z_{ij} I_j I_j^*
\end{aligned}$$

The first term is the complex power consumed by the load. The second term is the complex power injected at node j. The third term is the loss on the line. Now we can write:

$$S_i = s_i + \sum_j S_j + \sum_j \left(r_{ij} + x_{ij} \right) \frac{P_{ij}^2 + Q_{ij}^2}{V_j^2} \tag{26}$$

If we choose to neglect the loss term, we can see how this equation easily separates into real and reactive power:

$$P_i \approx p_i + \sum_j P_j \tag{27}$$

$$Q_i \approx q_i + \sum_j Q_j \tag{28}$$

Now, we consider the voltage magnitudes across nodes in the system.

$$\begin{aligned}
|V_i|^2 &= V_i V_i^* \\
&= \left(V_j + Z_{ij} I_j \right) \left(V_j^* + I_j^* Z_{ij}^* \right) \\
&= |V_j|^2 + 2Re[V_j I_j^* Z_{ij}^*] + Z_{ij} I_j I_j^* Z_{ij}^* \\
&= |V_j|^2 + 2Re[S_j Z_{ij}^*] + \left(r_{ij} + j x_{ij} \right) \frac{S_{ij}^*}{V_j^*} \frac{S_{ij}}{V_j} \left(r_{ij} - j x_{ij} \right) \\
&= |V_j|^2 + 2Re[\left(P_j + j Q_j \right) \left(r_{ij} - j x_{ij} \right)] + \left(r_{ij}^2 + x_{ij}^2 \right) \frac{(P_{ij} - j Q_{ij})(P_{ij} + j Q_{ij})}{V_j^* V_j} \\
&= |V_j|^2 + 2Re[P_j r_{ij} - j P_j x_{ij} + j Q_j r_{ij} + Q_j x_{ij}] + \left(r_{ij}^2 + x_{ij}^2 \right) \frac{P_{ij}^2 + Q_{ij}^2}{|V_j|^2} \\
&= |V_j|^2 + 2 r_{ij} P_j + 2 x_{ij} Q_j + \left(r_{ij}^2 + x_{ij}^2 \right) \frac{P_{ij}^2 + Q_{ij}^2}{|V_j|^2}
\end{aligned}$$

We can define the voltage magnitudes at each node in the network with reference to the nodes immediately upstream and downstream of the target node. The last term accounts for the losses in the system. The signs of the real and reactive power terms depend on whether power is being injected into or demanded out of the system.

$$|V_i|^2 = |V_j|^2 + 2 r_{ij} P_j + 2 x_{ij} Q_j + \left(r_{ij}^2 + x_{ij}^2 \right) \frac{P_{ij}^2 + Q_{ij}^2}{|V_j|^2} \tag{29}$$

We can therefore write expressions for the voltage, power, and reactive power at each node in terms of the nodes that are immediately downstream. Solving this system of equations allows us to determine these indicators throughout the distribution feeder. For example, if nodes j and k are the only nodes immediately downstream of node i, we would write (neglecting losses for now):

$$|V_i|^2 = |V_j|^2 + 2r_{ij}P_j + 2x_{ij}Q_j$$
$$|V_i|^2 = |V_k|^2 + 2r_{ik}P_k + 2x_{ik}Q_k$$
$$P_i = p_i + P_j + P_k$$
$$Q_i = q_i + Q_j + Q_k$$

This approach allows us to determine the voltage at each node with reference to the original source voltage. For a distribution feeder with n nodes, we have:

$$V = V_0 - 2Rp - 2Xq \tag{30}$$

Where:

$$V = \begin{bmatrix} |V_1|^2 \\ |V_2|^2 \\ \vdots \\ |V_n|^2 \end{bmatrix}, \qquad V_0 = \begin{bmatrix} |V_0|^2 \\ |V_0|^2 \\ \vdots \\ |V_0|^2 \end{bmatrix}, \qquad p = \begin{bmatrix} p_1 \\ p_2 \\ \vdots \\ p_n \end{bmatrix}, \qquad q = \begin{bmatrix} q_1 \\ q_2 \\ \vdots \\ q_n \end{bmatrix}, \qquad R, X \in \mathbb{R}^{n \times n}$$

And:

$$R_{ij} = \sum_{(\hat{i},\hat{j}) \in E_i \cap E_j} r_{\hat{i},\hat{j}}$$

Where E_i is the set containing the line segments that connect node 0 to node i.

Equations 27, 28, 29, and 30 allow us to fully define the parameters of interest (except losses) throughout a distribution system.

REFERENCES

[1] M. Coddington, B. Mather, B. Kroposki, K. Lynn, A. Razon, A. Ellis, R. Hill, T. Key, K. Nicole, J. W. Smith, National Renewable Energy Laboratory, US DOE, and Electric Power Research Institute, "Updating Interconnection Screens for PV System Integration," Tech. Rep., 2012. [Online]. Available: http://www.osti.gov/servlets/purl/1036038/

[2] M. A. Cohen and D. S. Callaway, "Effects of distributed PV generation on California's distribution system, Part 1: Engineering simulations," *Solar Energy*, vol. 128, pp. 126–138, 2016. [Online]. Available: http://linkinghub.elsevier.com/retrieve/pii/S0038092X16000049

[3] R. A. Walling, R. Saint, R. C. Dugan, J. Burke, and L. A. Kojovic, "Summary of distributed resources impact on power delivery systems," *IEEE Transactions on Power Delivery*, vol. 23, no. 3, pp. 1636–1644, 2008.

[4] A. Hoke and P. Komor, "Maximizing the Benefits of Distributed Photovoltaics," *Electricity Journal*, vol. 25, no. 3, pp. 55–67, 2012. [Online]. Available: https://www.sciencedirect.com/science/article/pii/S1040619012000589

[5] J. Weaver, "The Golden State is officially a third renewable, and it's not stopping there," *PV Magazine*, feb 2019. [Online]. Available: https://pv-magazine-usa.com/2019/02/25/golden-state-is-officially-a-third-renewable-growth-not-stopping-though/

[6] California Public Utilities Commission, "California's Distributed Energy Resources Action Plan: Aligning Vision and Action," pp. 1–12, may 2017. [Online]. Available: https://www.cpuc.ca.gov/uploadedFiles/CPUC_Public_Website/Content/About_Us/Organization/Commissioners/Michael_J._Picker/DER Action Plan (5-3-17) CLEAN.pdf https://www.cpuc.ca.gov/General.aspx?id=6442458159

[7] S. Stanfield and Interstate Renewable Energy Council, "Key Lessons from the California Integrated Capacity Analysis," *Interstate Renewable Energy Council*, pp. 1–6, 2018. [Online]. Available: https://irecusa.org/2018/10/key-lessons-from-the-california-integrated-capacity-analysis/

[8] S. Borenstein, "Private Net Benefits of Residential Solar PV: The Role of Electricity Tariffs, Tax Incentives, and Rebates," *Journal of the Association of Environmental and Resource Economists*, vol. 4, no. S1, 2017. [Online]. Available: https://www.journals.uchicago.edu/doi/10.1086/691978 http://www.nber.org/papers/w21342%5Cnhttp://www.nber.org/papers/w21342.pdf

[9] Go Solar California, "Statistics and Charts: NEM Solar PV," 2019. [Online]. Available: https://www.californiadgstats.ca.gov/charts/

[10] S. Weissman, A. M. Brockway, and Center for Sustainable Energy, "Community Solar in California: A Missed Opportunity," Tech. Rep. February, 2018. [Online]. Available: https://energycenter.org/sites/default/files/docs/nav/policy/resources/Community_Solar_in_California-A_Missed_Opportunity.pdf

[11] D. Feldman, A. M. Brockway, E. Ulrich, R. Margolis, and National Renewable Energy Laboratory, "Shared Solar: Current Landscape, Market Potential, and the Impact of Federal Securities Regulation," Tech. Rep. April, 2015. [Online]. Available: https://www.nrel.gov/docs/fy15osti/63892.pdf

[12] Office of Energy Efficiency & Renewable Energy, "Commercial and Residential Hourly Load Profiles for all TMY3 Locations in the United States," 2013. [Online]. Available: https://openei.org/doe-opendata/dataset/commercial-and-residential-hourly-load-profiles-for-all-tmy3-locations-in-the-united-states

[13] W. Gorman, S. Jarvis, and D. Callaway, "Should I Stay Or Should I Go? The importance of electricity rate design for household defection from the power grid," *Applied Energy*, no. (under review), 2019.

[14] California Energy Commission, "California Energy Maps: California Building Climate Zone Areas," California Energy Commission, Sacramento, CA, Tech. Rep., 2017. [Online]. Available: https://ww2.energy.ca.gov/maps/renewable/building_climate_zones.html

[15] Pacific Energy Center, "California Climate Zones and Bioclimactic Design," Tech. Rep. October, 2006. [Online]. Available: https://www.pge.com/includes/docs/pdfs/about/edusafety/training/pec/toolbox/arch/climate/california_climate_zones_01-16.pdf

[16] A. P. Dobos and National Renewable Energy Laboratory, "PVWatts Version 5 Manual," *National Renewable Energy Laboratory*, no. September, 2014. [Online]. Available: https://www.nrel.gov/docs/fy14osti/62641.pdf

[17] National Renewable Energy Laboratory, "PVWatts Calculator," 2016. [Online]. Available: https://pvwatts.nrel.gov/pvwatts.php

[18] M. Sengupta, Y. Xie, A. Lopez, A. Habte, G. Maclaurin, and J. Shelby, "The National Solar Radiation Data Base (NSRDB)," *Renewable and Sustainable Energy Reviews*, vol. 89, no. March, pp. 51–60, 2018. [Online]. Available: https://www.sciencedirect.com/science/article/pii/S136403211830087X

[19] G. Barbose and N. R. Darghouth, "Tracking the Sun: Pricing and Design Trends for Distributed Photovoltaic Systems in the United States, 2019 Edition," Lawrence Berkeley National Laboratory, Berkeley, CA, Tech. Rep., sep 2019. [Online]. Available: https://emp.lbl.gov/tracking-the-sun/

[20] IEEE PES Test Feeder Working Group, "1992 Test Feeder Cases," 1992. [Online]. Available: http://sites.ieee.org/pes-testfeeders/resources/

[21] K. P. Schneider, B. A. Mather, B. C. Pal, C.-W. Ten, G. J. Shirek, H. Zhu, J. C. Fuller, J. L. R. Pereira, L. F. Ochoa, L. R. de Araujo, R. C. Dugan, S. Matthias, S. Paudyal, T. E. McDermott, and W. Kersting, "Analytic Considerations and Design Basis for the IEEE

Distribution Test Feeders," *IEEE Transactions on Power Systems*, vol. 33, no. 3, pp. 3181–3188, may 2018. [Online]. Available: https://ieeexplore.ieee.org/document/8063903/

[22] National Electrical Manufacturers Association, "American National Standard for Electric power systems and equipment—Voltage ratings (60 Hertz)," American National Standards Institute, Inc., Tech. Rep., jun 2016. [Online]. Available: https://www.nema.org/Standards/Pages/American-National-Standard-for-Electric-Power-Systems-and-Equipment-Voltage-Ratings.aspx

[23] Y. Liu, J. Bebic, B. Kroposki, J. de Bedout, and W. Ren, "Distribution System Voltage Performance Analysis for High-Penetration Photovoltaics," in *IEEE Energy2030*, no. February, Atlanta, GA, 2008.

[24] M. Liu, P. K. Phanivong, and D. S. Callaway, "Decentralized Charging Control of Electric Vehicles in Residential Distribution Networks," *IEEE Transactions on Control Systems Technology*, pp. 1–15, 2017. [Online]. Available: https://ieeexplore.ieee.org/document/8118112/

[25] K. Turitsyn, P. Sulc, and M. Chertkov, "Distributed control of reactive power flow in a radial distribution circuit with high photovoltaic penetration," in *IEEE PES General Meeting*. Providence, RI: IEEE, 2010, pp. 1–6. [Online]. Available: https://ieeexplore.ieee.org/document/5589663

[26] V. Kekatos, "Lecture 12: DistFlow and LinDistFlow," Blacksburg, VA, pp. 1–30. [Online]. Available: https://www.faculty.ece.vt.edu/kekatos/pdsa.php

[27] R. A. Jabr, "Radial Distribution Load Flow Using Conic Programming," *IEEE Transactions on Power Systems*, vol. 21, no. 3, pp. 1458–1459, 2006. [Online]. Available: https://ieeexplore.ieee.org/document/1664986

[28] D. K. Molzahn and I. A. Hiskens, "A Survey of Relaxations and Approximations of the Power Flow Equations," *Foundations and Trends in Electric Energy Systems*, vol. 4, no. 1-2, pp. 1–221, 2019. [Online]. Available: https://www.nowpublishers.com/article/Details/EES-012

[29] S. Bansal and C.-y. Shih, "Convex Relaxation of Optimal Power Flow Problem," Project Report, UC Berkeley. [Online]. Available: https://people.eecs.berkeley.edu/ somil/Papers/project_report.pdf

[30] R. Seguin, J. Woyak, D. Costyk, J. Hambrick, B. Mather, and National Renewable Energy Laboratory, "High-Penetration PV Integration Handbook for Distribution Engineers," Tech. Rep., 2016.

[31] J. Löfberg, "YALMIP: A Toolbox for Modeling and Optimization in Matlab," in *IEEE International Symposium on Computer-Aided Control System Design*, Taipei, Taiwan, 2004. [Online]. Available: https://yalmip.github.io/